



1  
2  
3 **Mitochondrial respiratory states and rates:**  
4 **Building blocks of mitochondrial physiology Part 1**  
5

6 **COST Action CA15203 MitoEAGLE preprint Version: 2018-10-17(44)**  
7

8 Corresponding author: Gnaiger E

9 Co-authors:

10 Aasander Frostner E, Abumrad NA, Acuna-Castroviejo D, Adams SH, Ahn B, Ali SS, Alves MG,  
11 Amati F, Amoedo ND, Andreadou I, Aral C, Arandarčikaitė O, Arnould T, Avram VF, Bailey DM,  
12 Bajpeyi S, Bakker BM, Bastos Sant'Anna Silva AC, Battino M, Bazil J, Beard DA, Bednarczyk P,  
13 Bello F, Ben-Shachar D, Bergdahl A, Berge RK, Bernardi P, Bishop D, Blier PU, Blindheim DF,  
14 Boetker HE, Boros M, Borsheim E, Borutaitė V, Bouillaud F, Bouitbir J, Boushel RC, Bovard J,  
15 Breton S, Brown DA, Brown GC, Brown RA, Brozinick JT, Buettner GR, Burtscher J, Calabria E,  
16 Calbet JA, Calzia E, Cannon DT, Cano Sanchez M, Canto AC, Cardoso LHD, Carvalho E, Casado  
17 Pinna M, Cassina AM, Castro L, Cavalcanti-de-Albuquerque JP, Cervinkova Z, Chabi B, Chakrabarti  
18 L, Chaurasia B, Chen Q, Chicco AJ, Chinopoulos C, Chowdhury SK, Cizmarova B, Clementi E, Coen  
19 PM, Coker RH, Collin A, Crisóstomo L, Dambrova M, Danhelovska T, Darveau CA, Das AM, Dash  
20 RK, Davidova E, Davis MS, De Goede P, De Palma C, Dembinska-Kiec A, Devaux Y, Di Marcello  
21 M, Dias TR, Distefano G, Doermann N, Doerrier C, Donnelly C, Drahota Z, Dubouchaud H, Duchon  
22 MR, Dumas JF, Durham WJ, Dymkowska D, Dyrstad SE, Dyson A, Dzialowski EM, Ehinger J, Elmer  
23 E, Endlicher R, Engin AB, Escames G, Ezrova Z, Falk MJ, Fell DA, Ferdinandy P, Ferko M, Ferreira  
24 JCB, Ferreira R, Fessel JP, Filipovska A, Fisar Z, Fischer M, Fisher G, Fisher JJ, Ford E, Fornaro M,  
25 Galina A, Galkin A, Galli GL, Gan Z, Ganetzky R, Garcia-Roves PM, Garcia-Souza LF, Garipi E,  
26 Garlid KD, Garrabou G, Garten A, Gastaldelli A, Genova ML, Giovarelli M, Gonzalez-Armenta JL,  
27 Gonzalo H, Goodpaster BH, Gorr TA, Gourlay CW, Granata C, Grefte S, Guarch ME, Gueguen N,  
28 Gumeni S, Haas CB, Haavik J, Haendeler J, Hamann A, Han J, Han WH, Hancock CR, Hand SC,  
29 Hargreaves IP, Harrison DK, Hausenloy DJ, Heales SJR, Hellgren KT, Hepple RT, Hernansanz-  
30 Agustin P, Hickey AJ, Hoel F, Holland OJ, Holloway GP, Hoppel CL, Hoppel F, Houstek J, Huete-  
31 Ortega M, Iglesias-Gonzalez J, Irving BA, Iyer S, Jackson CB, Jadiya P, Jang DH, Jang YC, Janowska  
32 J, Jansen-Dürr P, Jansone B, Jarmuszkiewicz W, Jespersen NR, Jha RK, Jurczak MJ, Jurk D, Kaambre  
33 T, Kaczor JJ, Kainulainen H, Kandel SM, Kane DA, Kappler L, Karabatsiakakis A, Karkucinska-  
34 Wieckowska A, Keijer J, Keller MA, Keppner G, Khamoui AV, Kilbaugh T, Klepinin A, Klingenspor  
35 M, Komlodi T, Koopman WJH, Kopitar-Jerala N, Kowaltowski AJ, Kozlov AV, Krajcova A, Krako  
36 Jakovljevic N, Kristal BS, Kuang J, Kucera O, Kuka J, Kwak HB, Kwast K, Laasmaa M, Labieniec-  
37 Watala M, Lai N, Land JM, Lane N, Laner V, Lanza IR, Larsen TS, Lavery GG, Lazou A, Lee HK,  
38 Leeuwenburgh C, Lemieux H, Lenaz G, Lerfall J, Li PA, Liepins E, Liu J, Lucchinetti E, Macedo MP,  
39 MacMillan-Crow LA, Makarova E, Makrecka-Kuka M, Malik AN, Markova M, Martin DS, Mazat JP,  
40 McKenna HT, Menze MA, Merz T, Meszaros AT, Methner A, Michalak S, Moellering DR, Moisoï N,  
41 Molina AJA, Montaigne D, Moore AL, Moreau K, Moreno-Sánchez R, Moreira BP, Mracek T,  
42 Muntane J, Muntean DM, Murray AJ, Nair KS, Nehlin JO, Nemeč M, Neuffer PD, Neuzil J, Neviere  
43 R, Newsom S, Nozickova K, O'Brien KA, O'Gorman D, Olgar Y, Oliveira MF, Oliveira MT, Oliveira  
44 PF, Oliveira PJ, Orynbayeva Z, Osiewacz HD, Ounpuu L, Pak YK, Pallotta ML, Palmeira CM,  
45 Parajuli N, Passos JF, Passrugger M, Patel HH, Pavlova N, Pecina P, Pelnena D, Pereira da Silva Grilo  
46 da Silva F, Perez Valencia JA, Pesta D, Petit PX, Pettersen IKN, Pichaud N, Piel S, Pietka TA, Pino  
47 MF, Pirkmajer S, Porter C, Porter RK, Pranger F, Prochownik EV, Pulinilkunnil T, Puskarich MA,  
48 Puurand M, Quijano C, Radenkovic F, Radi R, Ramzan R, Rattan S, Reboredo P, Rich PR, Renner-

49 Sattler K, Rial E, Robinson MM, Roden M, Rodríguez-Enriquez S, Rohlena J, Rolo AP, Ropelle ER,  
 50 Røslund GV, Rossignol R, Rossiter HB, Rubelj I, Rybacka-Mossakowska J, Saada A, Safaei Z, Salin  
 51 K, Salvadego D, Sandi C, Sanz A, Sazanov LA, Scatena R, Schartner M, Scheibye-Knudsen M,  
 52 Schilling JM, Schlattner U, Schönfeld P, Schulz R, Schwarzer C, Scott GR, Shabalina IG, Sharma P,  
 53 Sharma V, Shevchuk I, Siewiera K, Silber AM, Silva AM, Sims CA, Singer D, Skolik R, Smenes BT,  
 54 Smith J, Soares FAA, Sobotka O, Sokolova I, Sonkar VK, Sowton AP, Sparagna GC, Sparks LM,  
 55 Spinazzi M, Stankova P, Starr J, Stary C, Stelfa G, Stiban J, Stier A, Stocker R, Sumbalova Z,  
 56 Suravajhala P, Svalbe B, Swerdlow RH, Swiniuch D, Szabo I, Szewczyk A, Szibor M, Tanaka M,  
 57 Tandler B, Tarnopolsky MA, Tausan D, Tavernarakis N, Tepp K, Thyfault JP, Tomar D, Towheed A,  
 58 Tretter L, Trifunovic A, Trivigno C, Tronstad KJ, Trougakos IP, Tuncay E, Turan B, Tyrrell DJ,  
 59 Urban T, Valentine JM, Vendelin M, Vercesi AE, Victor VM, Viel C, Vieyra A, Vilks K, Villena JA,  
 60 Vinogradov AD, Viscomi C, Vitorino RMP, Vogt S, Volani C, Volska K, Votion DM, Vujacic-Mirski  
 61 K, Wagner BA, Ward ML, Warnsmann V, Wasserman DH, Watala C, Wei YH, Wickert A,  
 62 Wieckowski MR, Williams C, Winwood-Smith H, Wohlgemuth SE, Wohlwend M, Wolff J, Wüst  
 63 RCI, Yokota T, Zablocki K, Zaugg K, Zaugg M, Zdrzilova L, Zhang Y, Zhang YZ, Zíková A,  
 64 Zischka H, Zorzano A, Zvejniece L

65  
 66 **Updates and discussion:**

67 [http://www.mitoeagle.org/index.php/MitoEAGLE\\_preprint\\_2018-02-08](http://www.mitoeagle.org/index.php/MitoEAGLE_preprint_2018-02-08)

68  
 69 Correspondence: Gnaiger E

70 *Chair COST Action CA15203 MitoEAGLE* – <http://www.mitoeagle.org>

71 *Department of Visceral, Transplant and Thoracic Surgery, D. Swarovski Research Laboratory,*

72 *Medical University of Innsbruck, Innrain 66/4, A-6020 Innsbruck, Austria*

73 *Email: mitoeagle@i-med.ac.at; Tel: +43 512 566796, Fax: +43 512 566796 20*

74



75	<b>Table of contents</b>
76	
77	<b>Abstract</b>
78	<b>Executive summary</b>
79	<b>1. Introduction</b> – Box 1: In brief: Mitochondria and Bioblasts
80	<b>2. Coupling states and rates in mitochondrial preparations</b>
81	2.1. <i>Cellular and mitochondrial respiration</i>
82	2.1.1. Aerobic and anaerobic catabolism and ATP turnover
83	2.1.2. Specification of biochemical dose
84	2.2. <i>Mitochondrial preparations</i>
85	2.3. <i>Electron transfer pathways</i>
86	2.4. <i>Respiratory coupling control</i>
87	2.4.1. Coupling
88	2.4.2. Phosphorylation, P <sub>s</sub> , and P <sub>s</sub> /O <sub>2</sub> ratio
89	2.4.3. Uncoupling
90	2.5. <i>Coupling states and respiratory rates</i>
91	2.5.1. <b>LEAK-state</b>
92	2.5.2. <b>OXPHOS-state</b>
93	2.5.3. <b>Electron transfer-state</b>
94	2.5.4. ROX state and <i>Rox</i>
95	2.5.5. Quantitative relations
96	2.5.6. The steady-state
97	2.6. <i>Classical terminology for isolated mitochondria</i>
98	2.6.1. State 1
99	2.6.2. State 2
100	2.6.3. State 3
101	2.6.4. State 4
102	2.6.5. State 5
103	2.7. <i>Control and regulation</i>
104	<b>3. What is a rate?</b> – Box 2: Metabolic flows and fluxes: vectorial, vectorial, and scalar
105	<b>4. Normalization of rate per sample</b>
106	4.1. <i>Flow: per object</i>
107	4.1.1. Number concentration
108	4.1.2. Flow per object
109	4.2. <i>Size-specific flux: per sample size</i>
110	4.2.1. Sample concentration
111	4.2.2. Size-specific flux
112	4.3. <i>Marker-specific flux: per mitochondrial content</i>
113	4.3.1. Mitochondrial concentration and mitochondrial markers
114	4.3.2. mt-Marker-specific flux
115	<b>5. Normalization of rate per system</b>
116	5.1. <i>Flow: per chamber</i>
117	5.2. <i>Flux: per chamber volume</i>
118	5.2.1. System-specific flux
119	5.2.2. Advancement per volume
120	<b>6. Conversion of units</b>
121	<b>7. Conclusions</b> – Box 3: Recommendations for studies with mitochondrial preparations
122	<b>References</b>
123	<b>Supplement</b>
124	S1. Manuscript phases and versions - an open-access approach
125	S2. Authors
126	S3. Joining COST Actions
127	

128 **Abstract** As the knowledge base and importance of mitochondrial physiology to human health expands,  
 129 the necessity for harmonizing the terminology concerning mitochondrial respiratory states and rates has  
 130 become increasingly apparent. The chemiosmotic theory establishes the mechanism of energy  
 131 transformation and coupling in oxidative phosphorylation. The unifying concept of the protonmotive  
 132 force provides the framework for developing a consistent theoretical foundation of mitochondrial  
 133 physiology and bioenergetics. We follow IUPAC guidelines on terminology in physical chemistry,  
 134 extended by considerations on open systems and thermodynamics of irreversible processes. The  
 135 concept-driven constructive terminology incorporates the meaning of each quantity and aligns concepts  
 136 and symbols to the nomenclature of classical bioenergetics. We endeavour to provide a balanced view  
 137 on mitochondrial respiratory control and a critical discussion on reporting data of mitochondrial  
 138 respiration in terms of metabolic flows and fluxes. Uniform standards for evaluation of respiratory states  
 139 and rates will ultimately contribute to reproducibility between laboratories and thus support the  
 140 development of databases of mitochondrial respiratory function in species, tissues, and cells. Clarity of  
 141 concept and consistency of nomenclature facilitate effective transdisciplinary communication,  
 142 education, and ultimately further discovery.

143  
 144 *Keywords:* Mitochondrial respiratory control, coupling control, mitochondrial preparations,  
 145 protonmotive force, uncoupling, oxidative phosphorylation, OXPHOS, efficiency, electron transfer, ET;  
 146 electron transfer system, ETS; proton leak, LEAK, residual oxygen consumption, ROX, State 2, State  
 147 3, State 4, normalization, flow, flux, O<sub>2</sub>

148

---

## 149 **Executive summary**

150

151 In view of the broad implications for health care, mitochondrial researchers face an increasing  
 152 responsibility to disseminate their fundamental knowledge and novel discoveries to a wide range of  
 153 stakeholders and scientists beyond the group of specialists. This requires implementation of a commonly  
 154 accepted terminology within the discipline and standardization in the translational context. Authors,  
 155 reviewers, journal editors, and lecturers are challenged to collaborate with the aim to harmonize the  
 156 nomenclature in the growing field of mitochondrial physiology and bioenergetics, from evolutionary  
 157 biology and comparative physiology to mitochondrial medicine. In the present communication we focus  
 158 on the following concepts in mitochondrial physiology:

- 159 1. Aerobic respiration depends on the coupling of phosphorylation (ADP → ATP) to O<sub>2</sub> flux in  
 160 catabolic reactions. Coupling in oxidative phosphorylation is mediated by the translocation of  
 161 protons across the inner mitochondrial membrane through proton pumps generating or  
 162 utilizing the protonmotive force, that is maintained between the mitochondrial matrix and  
 163 intermembrane compartment or outer mitochondrial space. Compartmental coupling  
 164 distinguishes this vectorial component of oxidative phosphorylation from glycolytic  
 165 fermentation as the counterpart of cellular core energy metabolism (**Figure 1**). Cell respiration  
 166 is distinguished from fermentation: (1) Electron acceptors are supplied by external respiration  
 167 for the maintenance of redox balance, whereas fermentation is characterized by an internal  
 168 electron acceptor produced in intermediary metabolism. In aerobic cell respiration, redox  
 169 balance is maintained by O<sub>2</sub> as the electron acceptor. (2) Compartmental coupling in vectorial  
 170 oxidative phosphorylation contrasts to exclusively scalar substrate-level phosphorylation in  
 171 fermentation.
- 172 2. When measuring mitochondrial metabolism, the contribution of fermentation and other cytosolic  
 173 interactions must be excluded from analysis by disrupting the barrier function of the plasma  
 174 membrane. Selective removal or permeabilization of the plasma membrane yields  
 175 mitochondrial preparations—including isolated mitochondria, tissue and cellular  
 176 preparations—with structural and functional integrity. Subsequently, extra-mitochondrial  
 177 concentrations of fuel substrates, ADP, ATP, inorganic phosphate, and cations including H<sup>+</sup>  
 178 can be controlled to determine mitochondrial function under a set of conditions defined as  
 179 *coupling control states*. We strive to incorporate an easily recognized and understood, concept-  
 180 driven terminology of bioenergetics with explicit terms and symbols that define the nature of  
 181 respiratory states.
- 182 3. Mitochondrial coupling states are defined according to the control of respiratory oxygen flux by  
 183 the protonmotive force. Capacities of oxidative phosphorylation and electron transfer are

measured at kinetically saturating concentrations of fuel substrates, ADP and inorganic phosphate, and O<sub>2</sub>, or at optimal uncoupler concentrations, respectively, in the absence of Complex IV inhibitors such as NO, CO, or H<sub>2</sub>S. Respiratory capacity is a measure of the upper bound of the rate of respiration; it depends on the substrate type undergoing oxidation, and provides reference values for the diagnosis of health and disease, and for evaluation of the effects of Evolutionary background, Age, Gender and sex, Lifestyle and Environment.

### Figure 1. Internal and external respiration

Mitochondrial respiration is the oxidation of fuel substrates (electron donors) and reduction of O<sub>2</sub> catalysed by the electron transfer system, ETS: **(mt)** mitochondrial catabolic respiration; **(ce)** total cellular O<sub>2</sub> consumption; and **(ext)** external respiration. All chemical reactions,  $r$ , that consume O<sub>2</sub> in the cells of an organism, contribute to cell respiration,  $J_{rO_2}$ . In addition to mitochondrial catabolic respiration, O<sub>2</sub> is consumed by:

① Mitochondrial residual O<sub>2</sub> consumption, *Rox*. ② Non-mitochondrial O<sub>2</sub> consumption by catabolic reactions, particularly peroxisomal oxidases and microsomal cytochrome P450 systems. ③ Non-mitochondrial *Rox* by reactions unrelated to catabolism. ④ Extracellular *Rox*. ⑤ Aerobic microbial respiration. Bars are not at a quantitative scale.

**(mt) Mitochondrial catabolic respiration,**  $J_{kO_2}$ , is the O<sub>2</sub> consumption by the mitochondrial ETS excluding *Rox*.

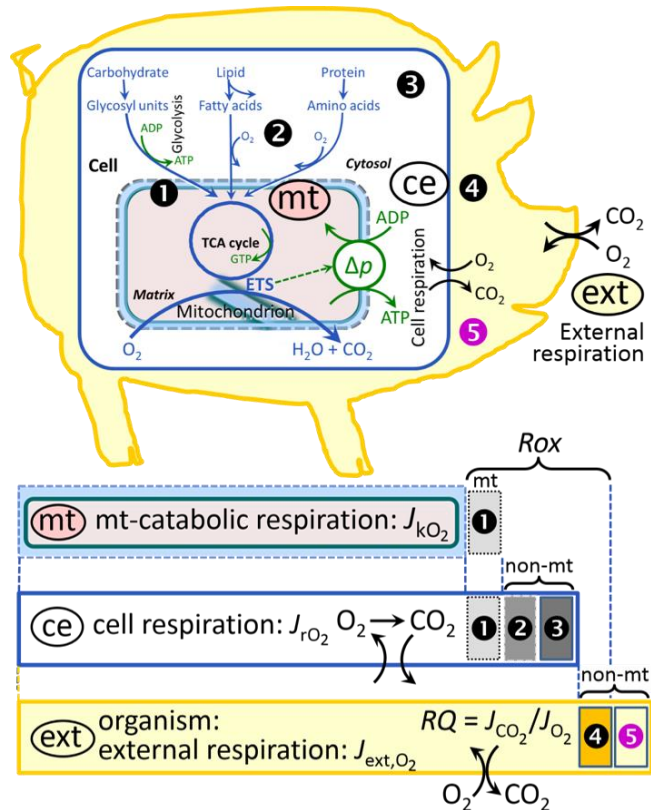
**(ce) Cell respiration,**  $J_{rO_2}$ , takes into account

internal O<sub>2</sub>-consuming reactions,  $r$ , including catabolic respiration and *Rox*. Catabolic cell respiration is the O<sub>2</sub> consumption associated with catabolic pathways in the cell, including mitochondrial catabolism in addition to peroxisomal and microsomal oxidation reactions (②).

**(ext) External respiration** balances internal respiration at steady-state, including extracellular *Rox* (④) and aerobic respiration by the microbiome (⑤). O<sub>2</sub> is transported from the environment across the respiratory cascade, *i.e.*, circulation between tissues and diffusion across cell membranes, to the intracellular compartment. The respiratory quotient,  $RQ$ , is the molar CO<sub>2</sub>/O<sub>2</sub> exchange ratio; when combined with the respiratory nitrogen quotient, N/O<sub>2</sub> (mol N given off per mol O<sub>2</sub> consumed), the  $RQ$  reflects the proportion of carbohydrate, lipid and protein utilized in cell respiration during aerobically balanced steady-states. Bicarbonate and CO<sub>2</sub> are transported in reverse to the extracellular milieu and the organismic environment. Hemoglobin provides the molecular paradigm for the combination of O<sub>2</sub> and CO<sub>2</sub> exchange, as do lungs and gills on the morphological level.

4. Incomplete tightness of coupling, *i.e.*, some degree of uncoupling relative to the substrate-dependent coupling stoichiometry, is a characteristic of energy-transformations across membranes. Uncoupling is caused by a variety of physiological, pathological, toxicological, pharmacological and environmental conditions that exert an influence not only on the proton leak and cation cycling, but also on proton slip within the proton pumps and the structural integrity of the mitochondria. A more loosely coupled state is induced by stimulation of mitochondrial superoxide formation and the bypass of proton pumps. In addition, the use of protonophores represents an experimental uncoupling intervention to assess the transition from a well-coupled to a noncoupled state of mitochondrial respiration.

5. Respiratory oxygen consumption rates have to be carefully normalized to enable meta-analytic studies beyond the question of a particular experiment. Therefore, all raw data on rates and variables for normalization should be published in an open access data repository.



240 Normalization of rates for: (1) the number of objects (cells, organisms); (2) the volume or  
 241 mass of the experimental sample; and (3) the concentration of mitochondrial markers in the  
 242 experimental chamber are sample-specific normalizations, which are distinguished from  
 243 system-specific normalization for the volume of the chamber (the measuring system).  
 244 6. The consistent use of terms and symbols will facilitate transdisciplinary communication and  
 245 support the further development of a collaborative database on bioenergetics and  
 246 mitochondrial physiology. The present considerations are focused on studies with  
 247 mitochondrial preparations. These will be extended in a series of reports on pathway control  
 248 of mitochondrial respiration, respiratory states in intact cells, and harmonization of  
 249 experimental procedures.  
 250

---

### 251 **Box 1: In brief – Mitochondria and Bioblasts**

252 *‘For the physiologist, mitochondria afforded the first opportunity for an experimental*  
 253 *approach to structure-function relationships, in particular those involved in active*  
 254 *transport, vectorial metabolism, and metabolic control mechanisms on a subcellular level’*  
 255 *(Ernster and Schatz 1981).*

256 Mitochondria are oxygen-consuming electrochemical generators that evolved from the endosymbiotic  
 257 alphaproteobacteria which integrated into a host cell related to Asgard Archaea (Margulis 1970; Lane  
 258 2005; Roger *et al.* 2017). They were described by Richard Altmann (1894) as ‘bioblasts’, which include  
 259 not only the mitochondria as presently defined, but also symbiotic and free-living bacteria. The word  
 260 ‘mitochondria’ (Greek mitos: thread; chondros: granule) was introduced by Carl Benda (1898).

261 Contrary to current textbook dogma, mitochondria form dynamic networks within eukaryotic  
 262 cells. Mitochondrial movement is supported by microtubules and morphology can change in response  
 263 to energy requirements of the cell via processes known as fusion and fission; these interactions allow  
 264 mitochondria to communicate within a network (Chan 2006). Mitochondria can even traverse cell  
 265 boundaries in a process known as horizontal mitochondrial transfer (Torralba *et al.* 2016). Another  
 266 defining characteristic of mitochondria is the double membrane. The mitochondrial inner membrane  
 267 (mtIM) forms dynamic tubular to disk-shaped cristae that separate the mitochondrial matrix, *i.e.*, the  
 268 negatively charged internal mitochondrial compartment, from the intermembrane space; the latter being  
 269 enclosed by the mitochondrial outer membrane (mtOM) and positively charged with respect to the  
 270 matrix. The mtIM contains the non-bilayer phospholipid cardiolipin, which is not present in any other  
 271 eukaryotic cellular membrane. Cardiolipin has many regulatory functions (Oemer *et al.* 2018); in  
 272 particular, it stabilizes and promotes the formation of respiratory supercomplexes (SC I<sub>n</sub>III<sub>n</sub>IV<sub>n</sub>), which  
 273 are supramolecular assemblies based upon specific and dynamic interactions between individual  
 274 respiratory complexes (Greggio *et al.* 2017; Lenaz *et al.* 2017). The fluidity of the mitochondrial  
 275 membrane is plastic and exerts an influence on the functional properties of proteins incorporated in  
 276 membranes (Waczulikova *et al.* 2007). Intracellular stress factors may cause shrinking or swelling of  
 277 the mitochondrial matrix, that can ultimately result in permeability transition.

278 Mitochondria are the structural and functional elementary components of cell respiration.  
 279 Mitochondrial respiration is the reduction of molecular oxygen by electron transfer coupled to  
 280 electrochemical proton translocation across the mtIM. In the process of oxidative phosphorylation  
 281 (OXPHOS), the catabolic reaction of oxygen consumption is electrochemically coupled to the  
 282 transformation of energy in the form of adenosine triphosphate (ATP; Mitchell 1961, 2011).  
 283 Mitochondria are the powerhouses of the cell which contain the machinery of the OXPHOS-pathways,  
 284 including transmembrane respiratory complexes (proton pumps with FMN, Fe-S and cytochrome *b*, *c*,  
 285 *aa*<sub>3</sub> redox systems); alternative dehydrogenases and oxidases; the coenzyme ubiquinone (Q); F-ATPase  
 286 or ATP synthase; the enzymes of the tricarboxylic acid cycle (TCA), fatty acid and amino acid oxidation;  
 287 transporters of ions, metabolites and co-factors; iron/sulphur cluster synthesis; and mitochondrial  
 288 kinases related to catabolic pathways. The mitochondrial proteome comprises over 1,200 proteins  
 289 (Calvo *et al.* 2015; 2017), mostly encoded by nuclear DNA (nDNA), with a variety of functions, many  
 290 of which are relatively well known (*e.g.*, proteins regulating mitochondrial biogenesis or apoptosis),  
 291 while others are still under investigation, or need to be identified (*e.g.*, permeability transition pore,  
 292 alanine transporter). Only recently has it been possible to use the mammalian mitochondrial proteome  
 293 to discover and characterize the genetic basis of mitochondrial diseases (Williams *et al.* 2016; Palmfeldt  
 294 and Bross 2017).

295 Numerous cellular processes are orchestrated by a constant crosstalk between mitochondria and  
 296 other cellular components. For example, the crosstalk between mitochondria and the endoplasmic  
 297 reticulum is involved in the regulation of calcium homeostasis, cell division, autophagy, differentiation,  
 298 and anti-viral signaling (Murley and Nunnari 2016). Mitochondria contribute to the formation of  
 299 peroxisomes, which are hybrids of mitochondrial and ER-derived precursors (Sugiura *et al.* 2017).  
 300 Cellular mitochondrial homeostasis (mitostasis) is maintained through regulation at transcriptional,  
 301 post-translational and epigenetic levels. Cell signalling modules contribute to homeostatic regulation  
 302 throughout the cell cycle or even cell death by activating proteostatic modules (*e.g.*, the ubiquitin-  
 303 proteasome and autophagy-lysosome/vacuole pathways; specific proteases like LON) and genome  
 304 stability modules in response to varying energy demands and stress cues (Quiros *et al.* 2016). Several  
 305 post-translational modifications, including acetylation and nitrosylation, are also capable of influencing  
 306 the bioenergetic response, with clinically significant implications for health and disease (Carrico *et al.*  
 307 2018).

308 Mitochondria of higher eukaryotes typically maintain several copies of their own circular genome  
 309 known as mitochondrial DNA (mtDNA; hundred to thousands per cell; Cummins 1998), which is  
 310 maternally inherited in humans. Biparental mitochondrial inheritance is documented in mammals, birds,  
 311 fish, reptiles and invertebrate groups, and is even the norm in some bivalve taxonomic groups (Breton  
 312 *et al.* 2007; White *et al.* 2008). The mitochondrial genome of the angiosperm *Amborella* contains a  
 313 record of six mitochondrial genome equivalents acquired by horizontal transfer of entire genomes, two  
 314 from angiosperms, three from algae and one from mosses (Rice *et al.* 2016). In unicellular organisms  
 315 (*i.e.*, protists) the structural organization of mitochondrial genomes is highly variable and includes  
 316 circular and linear DNA (Zikova *et al.* 2016). While some of the free-living flagellates exhibit the largest  
 317 known gene coding capacity (*e.g.* jakobid *Andalucia godoyi* mitochondrial DNA codes for 106 genes;  
 318 Burger *et al.* 2013), some protist groups (*e.g.* alveolates) possess mitochondrial genomes with only three  
 319 protein-coding genes and two rRNAs (Feagin *et al.* 2012). The complete loss of mitochondrial genome  
 320 is observed in highly reduced mitochondria of *Cryptosporidium* species (Liu *et al.* 2016). Reaching the  
 321 final extreme, the microbial eukaryote, oxymonad *Monocercomonoides*, has no mitochondrion  
 322 whatsoever and lacks all typical nuclear-encoded mitochondrial proteins demonstrating that while in  
 323 99% of organisms mitochondria play a vital role, this organelle is not indispensable (Karnkowska *et al.*  
 324 2016).

325 In vertebrates but not all invertebrates, mtDNA is compact (16.5 kB in humans) and encodes 13  
 326 protein subunits of the transmembrane respiratory Complexes CI, CIII, CIV and ATP synthase (F-  
 327 ATPase), 22 tRNAs, and two RNAs. Additional gene content has been suggested to include microRNAs,  
 328 piRNA, smithRNAs, repeat associated RNA, and even additional proteins (Duarte *et al.* 2014; Lee *et al.*  
 329 2015; Cobb *et al.* 2016). The mitochondrial genome requires nuclear-encoded mitochondrially  
 330 targeted proteins, *e.g.*, TFAM, for its maintenance and expression (Rackham *et al.* 2012). Both genomes  
 331 encode peptides of the membrane spanning redox pumps (CI, CIII and CIV) and F-ATPase, leading to  
 332 strong constraints in the coevolution of both genomes (Blier *et al.* 2001).

333 Given the multiple roles of mitochondria, it is perhaps not surprising that mitochondrial  
 334 dysfunction is associated with a wide variety of genetic and degenerative diseases. Robust mitochondrial  
 335 function is supported by physical exercise and caloric balance, and is central for sustained metabolic  
 336 health throughout life. Therefore, a more consistent set of definitions for mitochondrial physiology will  
 337 increase our understanding of the etiology of disease and improve the diagnostic repertoire of  
 338 mitochondrial medicine with a focus on protective medicine, lifestyle and healthy aging.

339 Mitochondrion is singular and mitochondria is plural. Abbreviation: mt, as generally used in  
 340 mtDNA.

341

342

343

## 344 1. Introduction

345

346 Mitochondria are the powerhouses of the cell with numerous physiological, molecular, and  
 347 genetic functions (**Box 1**). Every study of mitochondrial health and disease faces **Evolution, Age,**  
 348 **Gender and sex, Lifestyle, and Environment (MitoEAGLE)** as essential background conditions intrinsic  
 349 to the individual person or cohort, species, tissue and to some extent even cell line. As a large and  
 350 coordinated group of laboratories and researchers, the mission of the global MitoEAGLE Network is to

351 generate the necessary scale, type, and quality of consistent data sets and conditions to address this  
352 intrinsic complexity. Harmonization of experimental protocols and implementation of a quality control  
353 and data management system are required to interrelate results gathered across a spectrum of studies  
354 and to generate a rigorously monitored database focused on mitochondrial respiratory function. In this  
355 way, researchers from a variety of disciplines can compare their findings using clearly defined and  
356 accepted international standards.

357 With an emphasis on quality of research, published data can be useful far beyond the specific  
358 question of a particular experiment. For example, collaborative data sets support the development of  
359 open-access databases such as those for National Institutes of Health sponsored research in genetics,  
360 proteomics, and metabolomics. Indeed, enabling meta-analysis is the most economic way of providing  
361 robust answers to biological questions (Cooper *et al.* 2009). However, the reproducibility of quantitative  
362 results and databases depend on accurate measurements under strictly-defined conditions. Likewise,  
363 meaningful interpretation and comparability of experimental outcomes requires standardisation of  
364 protocols between research groups at different institutes. In addition to quality control, a conceptual  
365 framework is also required to standardise and homogenise terminology and methodology. Vague or  
366 ambiguous jargon can lead to confusion and may relegate valuable signals to wasteful noise. For this  
367 reason, measured values must be expressed in standard units for each parameter used to define  
368 mitochondrial respiratory function. A consensus on fundamental nomenclature and conceptual  
369 coherence, however, are missing in the expanding field of mitochondrial physiology. To fill this gap,  
370 the present communication provides an in-depth review on harmonization of nomenclature and  
371 definition of technical terms, which are essential to improve the awareness of the intricate meaning of  
372 current and past scientific vocabulary. This is important for documentation and integration into  
373 databases in general, and quantitative modelling in particular (Beard 2005).

374 In this review, we focus on coupling states and fluxes through metabolic pathways of aerobic  
375 energy transformation in mitochondrial preparations as a first step in the attempt to generate a  
376 conceptually-oriented nomenclature in bioenergetics and mitochondrial physiology. Respiratory control  
377 by fuel substrates and specific inhibitors of respiratory enzymes, coupling states of intact cells, and  
378 respiratory flux control ratios will be reviewed in subsequent communications, prepared in the frame of  
379 COST Action MitoEAGLE open to global bottom-up input.

380  
381

## 382 **2. Coupling states and rates in mitochondrial preparations**

383 *‘Every professional group develops its own technical jargon for talking about matters of critical*  
384 *concern ... People who know a word can share that idea with other members of their group, and*  
385 *a shared vocabulary is part of the glue that holds people together and allows them to create a*  
386 *shared culture’* (Miller 1991).

387

### 388 *2.1. Cellular and mitochondrial respiration*

389

390 **2.1.1. Aerobic and anaerobic catabolism and ATP turnover:** In respiration, electron transfer  
391 is coupled to the phosphorylation of ADP to ATP, with energy transformation mediated by the  
392 protonmotive force,  $\Delta p$  (**Figure 2**). Anabolic reactions are coupled to catabolism, both by ATP as the  
393 intermediary energy currency and by small organic precursor molecules as building blocks for  
394 biosynthesis. Glycolysis involves substrate-level phosphorylation of ADP to ATP in fermentation  
395 without utilization of  $O_2$ , studied mainly in intact cells and organisms. Many cellular fuel substrates are  
396 catabolized to acetyl-CoA or to glutamate, and further electron transfer reduces nicotinamide adenine  
397 dinucleotide to NADH or flavin adenine dinucleotide to FADH<sub>2</sub>. Subsequent mitochondrial electron  
398 transfer to  $O_2$  is coupled to proton translocation for the control of  $\Delta p$  and phosphorylation of ADP  
399 (**Figure 2B and 2C**). In contrast, extra-mitochondrial oxidation of fatty acids and amino acids proceeds  
400 partially in peroxisomes without coupling to ATP production: acyl-CoA oxidase catalyzes the oxidation  
401 of FADH<sub>2</sub> with electron transfer to  $O_2$ ; amino acid oxidases oxidize flavin mononucleotide FMNH<sub>2</sub> or  
402 FADH<sub>2</sub> (**Figure 2A**).

403



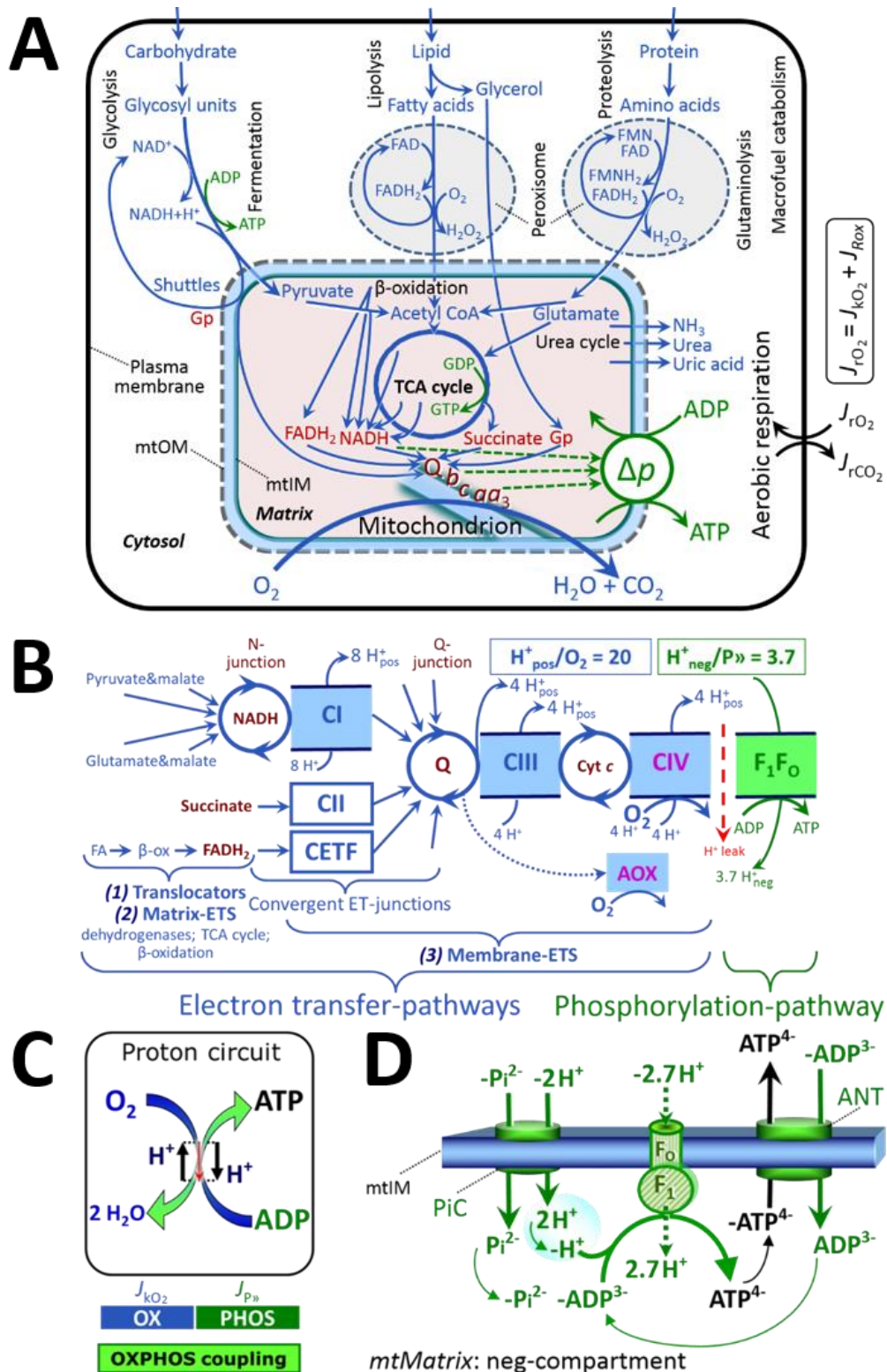


### Figure 2. Cell respiration and oxidative phosphorylation (OXPHOS)

Mitochondrial respiration is the oxidation of fuel substrates (electron donors) with electron transfer to  $O_2$  as the electron acceptor. For explanation of symbols see also **Figure 1**.

(A) Respiration of intact cells: Extra-mitochondrial catabolism of macromolecules and uptake of small molecules by the cell provide the mitochondrial fuel substrates. Dashed arrows indicate the connection between the redox proton pumps (respiratory Complexes CI, CIII and CIV) and the transmembrane  $\Delta p$ . Coenzyme Q (Q) and the cytochromes *b*, *c*, and *aa<sub>3</sub>* are redox systems of the mitochondrial inner membrane, mtIM. Glycerol-3-phosphate, Gp.

404  
405  
406  
407  
408  
409  
410  
411  
412

413 (B) Respiration in mitochondrial preparations: The mitochondrial electron transfer system  
 414 (ETS) is (1) fuelled by diffusion and transport of substrates across the mtOM and mtIM,  
 415 and in addition consists of the (2) matrix-ETS, and (3) membrane-ETS. Electron transfer  
 416 converges at the N-junction, and from CI, CII and electron transferring flavoprotein  
 417 complex (CETF) at the Q-junction. Unspecified arrows converging at the Q-junction  
 418 indicate additional ETS-sections with electron entry into Q through glycerophosphate  
 419 dehydrogenase, dihydro-orotate dehydrogenase, proline dehydrogenase, choline  
 420 dehydrogenase, and sulfide-ubiquinone oxidoreductase. The dotted arrow indicates the  
 421 branched pathway of oxygen consumption by alternative quinol oxidase (AOX). ET-  
 422 pathways are coupled to the phosphorylation-pathway. The  $H^+_{\text{pos}}/O_2$  ratio is the outward  
 423 proton flux from the matrix space to the positively (pos) charged vesicular compartment,  
 424 divided by catabolic  $O_2$  flux in the NADH-pathway. The  $H^+_{\text{neg}}/P_{\gg}$  ratio is the inward proton  
 425 flux from the inter-membrane space to the negatively (neg) charged matrix space, divided  
 426 by the flux of phosphorylation of ADP to ATP. These stoichiometries are not fixed due to  
 427 ion leaks and proton slip. Modified from Lemieux *et al.* (2017) and Rich (2013).  
 428 (C) OXPHOS coupling:  $O_2$  flux through the catabolic ET-pathway,  $J_{kO_2}$ , is coupled  
 429 by the  $H^+$  circuit to flux through the phosphorylation-pathway of ADP to ATP,  $J_{P_{\gg}}$ .  
 430 (D) Chemiosmotic phosphorylation-pathway catalyzed by the proton pump  $F_1F_0$ -ATPase  
 431 (F-ATPase, ATP synthase), adenine nucleotide translocase (ANT), and inorganic  
 432 phosphate carrier (PiC). The  $H^+_{\text{neg}}/P_{\gg}$  stoichiometry is the sum of the coupling  
 433 stoichiometry in the F-ATPase reaction ( $-2.7 H^+_{\text{pos}}$  from the positive intermembrane space,  
 434  $2.7 H^+_{\text{neg}}$  to the matrix, *i.e.*, the negative compartment) and the proton balance in the  
 435 translocation of  $ADP^{3-}$ ,  $ATP^{4-}$  and  $P_i^{2-}$ . Modified from Gnaiger (2014).  
 436

437 The plasma membrane separates the intracellular compartment including the cytosol, nucleus, and  
 438 organelles from the extracellular environment. The plasma membrane consists of a lipid bilayer with  
 439 embedded proteins and attached organic molecules that collectively control the selective permeability  
 440 of ions, organic molecules, and particles across the cell boundary. The intact plasma membrane prevents  
 441 the passage of many water-soluble mitochondrial substrates and inorganic ions—such as succinate,  
 442 adenosine diphosphate (ADP) and inorganic phosphate ( $P_i$ ), that must be precisely controlled at  
 443 kinetically-saturating concentrations for the analysis of mitochondrial respiratory capacities.  
 444 Respiratory capacities delineate, comparable to channel capacity in information theory (Schneider  
 445 2006), the upper bound of the rate of  $O_2$  consumption measured in defined respiratory states. Despite  
 446 the activity of solute carriers, *e.g.*, SLC13A3 and SLC20A2, which transport specific metabolites across  
 447 the plasma membrane of various cell types, the intact plasma membrane limits the scope of  
 448 investigations into mitochondrial respiratory function in intact cells.

449 **2.1.2. Specification of biochemical dose:** Substrates, uncouplers, inhibitors, and other chemical  
 450 reagents are titrated to analyse cellular and mitochondrial function. Nominal concentrations of these  
 451 substances are usually reported as initial amount of substance concentration [ $\text{mol}\cdot\text{L}^{-1}$ ] in the incubation  
 452 medium. When aiming at the measurement of kinetically saturated processes—such as OXPHOS-  
 453 capacities, the concentrations for substrates can be chosen according to the apparent equilibrium  
 454 constant,  $K_m'$ . In the case of hyperbolic kinetics, only 80% of maximum respiratory capacity is obtained  
 455 at a substrate concentration of four times the  $K_m'$ , whereas substrate concentrations of 5, 9, 19 and 49  
 456 times the  $K_m'$  are theoretically required for reaching 83%, 90%, 95% or 98% of the maximal rate  
 457 (Gnaiger 2001). Other reagents are chosen to inhibit or alter a particular process. The amount of these  
 458 chemicals in an experimental incubation is selected to maximize effect, avoiding unacceptable off-target  
 459 consequences that would adversely affect the data being sought. Specifying the amount of substance in  
 460 an incubation as nominal concentration in the aqueous incubation medium can be ambiguous (Doskey  
 461 *et al.* 2015), particularly for cations (TPP<sup>+</sup>; fluorescent dyes such as safranin, TMRM; Chowdhury *et al.*  
 462 2015) and lipophilic substances (oligomycin, uncouplers, permeabilization agents; Doerrier *et al.* 2018),  
 463 which accumulate in the mitochondrial matrix or in biological membranes, respectively. Generally,  
 464 dose/exposure can be specified per unit of biological sample, *i.e.*, (nominal moles of  
 465 xenobiotic)/(number of cells) [ $\text{mol}\cdot\text{cell}^{-1}$ ] or, as appropriate, per mass of biological sample [ $\text{mol}\cdot\text{kg}^{-1}$ ].  
 466 This approach to specification of dose/exposure provides a scalable parameter that can be used to design  
 467 experiments, help interpret a wide variety of experimental results, and provide absolute information that  
 468 allows researchers worldwide to make the most use of published data (Doskey *et al.* 2015).

## 469 2.2. Mitochondrial preparations

470

471 Mitochondrial preparations are defined as either isolated mitochondria, or tissue and cellular  
 472 preparations in which the barrier function of the plasma membrane is disrupted. Since this entails the  
 473 loss of cell viability, mitochondrial preparations are not studied *in vivo*. In contrast to isolated  
 474 mitochondria and tissue homogenate preparations, mitochondria in permeabilized tissues and cells are  
 475 *in situ* relative to the plasma membrane. When studying mitochondrial preparations, substrate-  
 476 uncoupler-inhibitor-titration (SUIT) protocols are used to establish respiratory coupling control states  
 477 (CCS) and pathway control states (PCS) that provide reference values for various output variables  
 478 (**Table 1**). Physiological conditions *in vivo* deviate from these experimentally obtained states; this is  
 479 because kinetically-saturating concentrations, *e.g.*, of ADP, oxygen (O<sub>2</sub>; dioxygen) or fuel substrates,  
 480 may not apply to physiological intracellular conditions. Further information is obtained in studies of  
 481 kinetic responses to variations in fuel substrate concentrations, [ADP], or [O<sub>2</sub>] in the range between  
 482 kinetically-saturating concentrations and anoxia (Gnaiger 2001).

483 The cholesterol content of the plasma membrane is high compared to mitochondrial membranes  
 484 (Korn 1969). Therefore, mild detergents—such as digitonin and saponin—can be applied to selectively  
 485 permeabilize the plasma membrane via interaction with cholesterol; this allows free exchange of organic  
 486 molecules and inorganic ions between the cytosol and the immediate cell environment, while  
 487 maintaining the integrity and localization of organelles, cytoskeleton, and the nucleus. Application of  
 488 permeabilization agents (mild detergents or toxins) leads to washout of cytosolic marker enzymes—  
 489 such as lactate dehydrogenase—and results in the complete loss of cell viability (tested by nuclear  
 490 staining using plasma membrane-impermeable dyes), while mitochondrial function remains intact  
 491 (tested by cytochrome *c* stimulation of respiration). Digitonin concentrations have to be optimized  
 492 according to cell type, particularly since mitochondria from cancer cells contain significantly higher  
 493 contents of cholesterol in both membranes (Baggetto and Testa-Perussini, 1990). For example, a dose  
 494 of digitonin of 8 fmol·cell<sup>-1</sup> (10 pg·cell<sup>-1</sup>; 10 μg·10<sup>-6</sup> cells) is optimal for permeabilization of endothelial  
 495 cells, and the concentration in the incubation medium has to be adjusted according to the cell density  
 496 applied (Doerrier *et al.* 2018). Respiration of isolated mitochondria remains unaltered after the addition  
 497 of low concentrations of digitonin or saponin. In addition to mechanical cell disruption during  
 498 homogenization of tissue, permeabilization agents may be applied to ensure permeabilization of all cells  
 499 in tissue homogenates.

500 Suspensions of cells permeabilized in the respiration chamber and crude tissue homogenates  
 501 contain all components of the cell at highly dilute concentrations. All mitochondria are retained in  
 502 chemically-permeabilized mitochondrial preparations and crude tissue homogenates. In the preparation  
 503 of isolated mitochondria, however, the mitochondria are separated from other cell fractions and purified  
 504 by differential centrifugation, entailing the loss of mitochondria at typical recoveries ranging from 30%  
 505 to 80% of total mitochondrial content (Lai *et al.* 2018). Using Percoll or sucrose density gradients to  
 506 maximize the purity of isolated mitochondria may compromise the mitochondrial yield or structural and  
 507 functional integrity. Therefore, mitochondrial isolation protocols need to be optimized according to each  
 508 study. The term mitochondrial preparation does neither include intact cells, nor submitochondrial  
 509 particles and further fractionation of mitochondrial components.

510

## 511 2.3. Electron transfer pathways

512

513 Mitochondrial electron transfer (ET) pathways are fuelled by diffusion and transport of substrates  
 514 across the mtOM and mtIM. In addition, the mitochondrial electron transfer system (ETS) consists of  
 515 the matrix-ETS, and membrane-ETS (**Figure 2B**). Upstream sections of ET-pathways converge at the  
 516 NADH-junction (N-junction). NADH is mainly generated in the tricarboxylic acid (TCA) cycle and is  
 517 oxidized by Complex I (CI), with further electron entry into the coenzyme Q-junction (Q-junction).  
 518 Similarly, succinate is formed in the TCA cycle and oxidized by CII to fumarate. CII is part of both the  
 519 TCA cycle and the ETS, and reduces FAD to FADH<sub>2</sub> with further reduction of ubiquinone to ubiquinol  
 520 downstream of the TCA cycle in the Q-junction. Thus FADH<sub>2</sub> is not a substrate but is the product of  
 521 CII, in contrast to erroneous metabolic maps shown in many publications. β-oxidation of fatty acids  
 522 (FA) generates FADH<sub>2</sub> as the substrate of electron transferring flavoprotein complex (ETF).

523 Selected mitochondrial catabolic pathways, *k*, of electron transfer from the oxidation of fuel  
 524 substrates to the reduction of O<sub>2</sub> are activated by depletion of endogenous substrates and addition of fuel

525 substrates to the mitochondrial respiration medium (**Figure 2B**). Substrate combinations and specific  
 526 inhibitors of ET-pathway enzymes are used to obtain defined pathway control states in mitochondrial  
 527 preparations (Gnaiger 2014).

528

#### 529 2.4. Respiratory coupling control

530

531 **2.4.1. Coupling:** In mitochondrial electron transfer, vectorial transmembrane proton flux is  
 532 coupled through the redox proton pumps CI, CIII and CIV to the catabolic flux of scalar reactions,  
 533 collectively measured as O<sub>2</sub> flux,  $J_{\text{KO}_2}$  (**Figure 2**). Thus mitochondria are elementary components of  
 534 energy transformation. Energy is a conserved quantity and cannot be lost or produced in any internal  
 535 process (First Law of thermodynamics). Open and closed systems can gain or lose energy only by  
 536 external fluxes—by exchange with the environment. Therefore, energy can neither be produced by  
 537 mitochondria, nor is there any internal process without energy conservation. Exergy or Gibbs energy  
 538 (‘free energy’) is the part of energy that can potentially be transformed into work under conditions of  
 539 constant temperature and pressure. *Coupling* is the interaction of an exergonic process (spontaneous,  
 540 negative exergy change) with an endergonic process (positive exergy change) in energy transformations  
 541 which conserve part of the exergy that would be irreversibly lost or dissipated in an uncoupled process.

542 Pathway control states (PCS) and coupling control states (CCS) are complementary, since  
 543 mitochondrial preparations depend on (1) an exogenous supply of pathway-specific fuel substrates and  
 544 oxygen, and (2) exogenous control of phosphorylation (**Figure 2**).

545 **2.4.2. Phosphorylation, P», and P»/O<sub>2</sub> ratio:** Phosphorylation in the context of OXPHOS is  
 546 defined as phosphorylation of ADP by P<sub>i</sub> to form ATP. On the other hand, the term phosphorylation is  
 547 used generally in many contexts, *e.g.*, protein phosphorylation. This justifies consideration of a symbol  
 548 more discriminating and specific than P as used in the P/O ratio (phosphate to atomic oxygen ratio),  
 549 where P indicates phosphorylation of ADP to ATP or GDP to GTP (**Figure 2**). We propose the symbol  
 550 P» for the endergonic (uphill) direction of phosphorylation ADP→ATP, and likewise the symbol P« for  
 551 the corresponding exergonic (downhill) hydrolysis ATP→ADP. P» refers mainly to electrontransfer  
 552 phosphorylation but may also involve substrate-level phosphorylation as part of the TCA cycle  
 553 (succinyl-CoA ligase; phosphoglycerate kinase) and phosphorylation of ADP catalyzed by pyruvate  
 554 kinase, and of GDP phosphorylated by phosphoenolpyruvate carboxykinase. Transphosphorylation is  
 555 performed by adenylate kinase, creatine kinase (mtCK), hexokinase and nucleoside diphosphate kinase.  
 556 In isolated mammalian mitochondria, ATP production catalyzed by adenylate kinase (2 ADP ↔ ATP +  
 557 AMP) proceeds without fuel substrates in the presence of ADP (Komlódi and Tretter 2017). Kinase  
 558 cycles are involved in intracellular energy transfer and signal transduction for regulation of energy flux.

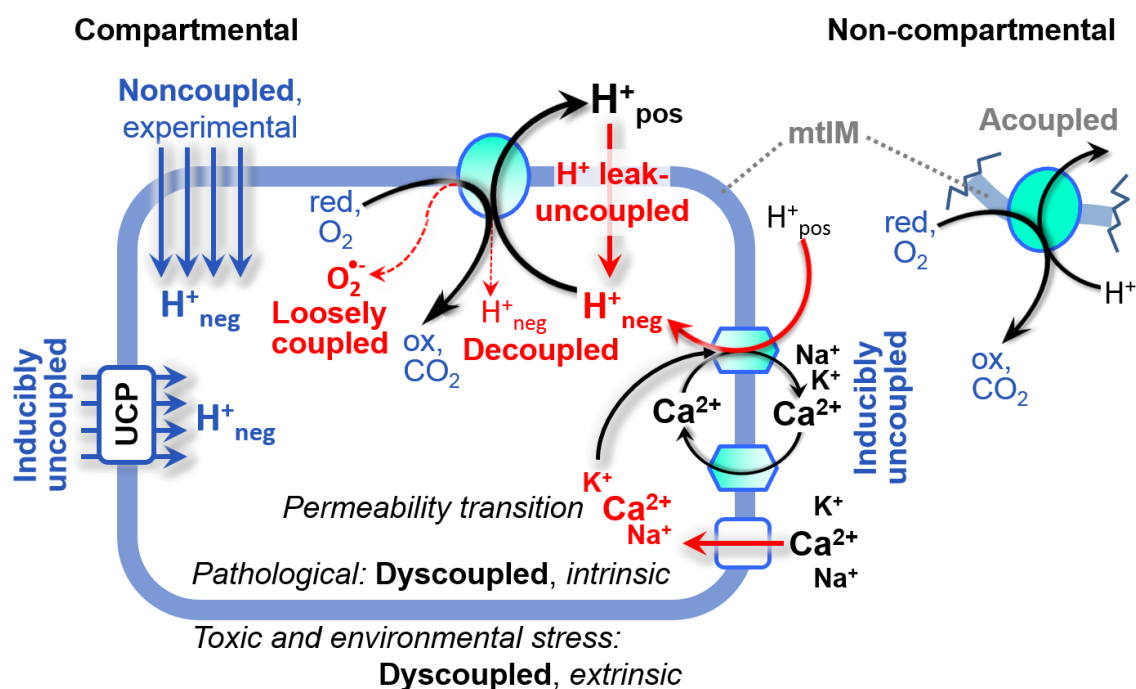
559 The P»/O<sub>2</sub> ratio (P»/4 e<sup>-</sup>) is two times the ‘P/O’ ratio (P»/2 e<sup>-</sup>) of classical bioenergetics. P»/O<sub>2</sub> is  
 560 a generalized symbol, not specific for determination of P<sub>i</sub> consumption (P<sub>i</sub>/O<sub>2</sub> flux ratio), ADP depletion  
 561 (ADP/O<sub>2</sub> flux ratio), or ATP production (ATP/O<sub>2</sub> flux ratio). The mechanistic P»/O<sub>2</sub> ratio—or P»/O<sub>2</sub>  
 562 stoichiometry—is calculated from the proton-to-O<sub>2</sub> and proton-to-phosphorylation coupling  
 563 stoichiometries (**Figure 2B**):

$$565 \quad \text{P}\gg/\text{O}_2 = \frac{H_{\text{pos}}^+/\text{O}_2}{H_{\text{neg}}^+/\text{P}\gg} \quad (1)$$

566  
 567 The H<sup>+</sup><sub>pos</sub>/O<sub>2</sub> coupling stoichiometry (referring to the full 4 electron reduction of O<sub>2</sub>) depends on the  
 568 relative involvement of the three coupling sites (respiratory Complexes CI, CIII and CIV) in the  
 569 catabolic ET-pathway from reduced fuel substrates (electron donors) to the reduction of O<sub>2</sub> (electron  
 570 acceptor). This varies with: (1) a bypass of CI by single or multiple electron input into the Q-junction;  
 571 and (2) a bypass of CIV by involvement of alternative oxidases, AOX, which are not expressed in  
 572 mammalian mitochondria.

573 The H<sup>+</sup><sub>pos</sub>/O<sub>2</sub> coupling stoichiometry equals 12 in the ET-pathways involving CIII and CIV as  
 574 proton pumps, increasing to 20 for the NADH-pathway through CI (**Figure 2B**), but a general consensus  
 575 on H<sup>+</sup><sub>pos</sub>/O<sub>2</sub> stoichiometries remains to be reached (Hinkle 2005; Wikström and Hummer 2012; Sazanov  
 576 2015). The H<sup>+</sup><sub>neg</sub>/P» coupling stoichiometry (3.7; **Figure 2B**) is the sum of 2.7 H<sup>+</sup><sub>neg</sub> required by the F-  
 577 ATPase of vertebrate and most invertebrate species (Watt *et al.* 2010) and the proton balance in the  
 578 translocation of ADP, ATP and P<sub>i</sub> (**Figure 2C**). Taken together, the mechanistic P»/O<sub>2</sub> ratio is calculated  
 579 at 5.4 and 3.3 for NADH- and succinate-linked respiration, respectively (Eq. 1). The corresponding  
 580 classical P»/O ratios (referring to the 2 electron reduction of 0.5 O<sub>2</sub>) are 2.7 and 1.6 (Watt *et al.* 2010),  
 581 in agreement with the measured P»/O ratio for succinate of 1.58 ± 0.02 (Gnaiger *et al.* 2000).

582



583

584

### Figure 3. Mechanisms of respiratory uncoupling

585 An intact mitochondrial inner membrane, mtIM, is required for vectorial, compartmental coupling.

586 'Acoupled' respiration is the consequence of structural disruption with catalytic activity of non-

587 compartmental mitochondrial fragments. Inducible uncoupling (e.g., by activation of UCP1) increases

588 LEAK respiration; experimentally noncoupled respiration provides an estimate of ET-capacity obtained

589 by titration of protonophores stimulating respiration to maximum  $O_2$  flux.  $H^+$  leak-uncoupled,

590 decoupled, and loosely coupled respiration are components of intrinsic uncoupling (Table 2).

591 Pathological dysfunction may affect all types of uncoupling, including permeability transition, causing

592 intrinsically dyscoupled respiration. Similarly, toxicological and environmental stress factors can cause

593 extrinsically dyscoupled respiration. Reduced fuel substrates, red; oxidized products, ox.

594

595

596 **2.4.3. Uncoupling:** The effective  $P_{\gg}/O_2$  flux ratio ( $Y_{P_{\gg}/O_2} = J_{P_{\gg}}/J_{KO_2}$ ) is diminished relative to the

597 mechanistic  $P_{\gg}/O_2$  ratio by intrinsic and extrinsic uncoupling or dyscoupling (Figure 3). Such

598 generalized uncoupling is different from switching to mitochondrial pathways that involve fewer than

599 three proton pumps ('coupling sites': Complexes CI, CIII and CIV), bypassing CI through multiple

600 electron entries into the Q-junction, or CIII and CIV through AOX (Figure 2B). Reprogramming of

601 mitochondrial pathways leading to different types of substrates being oxidized may be considered as a

602 switch of gears (changing the stoichiometry by altering the substrate that is oxidized) rather than

603 uncoupling (loosening the tightness of coupling relative to a fixed stoichiometry). In addition,  $Y_{P_{\gg}/O_2}$

604 depends on several experimental conditions of flux control, increasing as a hyperbolic function of [ADP]

605 to a maximum value (Gnaiger 2001).

606 Uncoupling of mitochondrial respiration is a general term comprising diverse mechanisms:

607 1. Proton leak across the mtIM from the pos- to the neg-compartment ( $H^+$  leak-uncoupled; Figure

608 3).

609 2. Cycling of other cations, strongly stimulated by permeability transition; comparable to the use of

610 protonophores, cation cycling is experimentally induced by valinomycin in the presence of  $K^+$ ;

611 3. Decoupling by proton slip in the redox proton pumps when protons are effectively not pumped

612 (CI, CIII and CIV) or are not driving phosphorylation (F-ATPase);

613 4. Loss of vesicular (compartmental) integrity when electron transfer is acoupled;

614 5. Electron leak in the loosely coupled univalent reduction of  $O_2$  to superoxide ( $O_2^{\bullet -}$ ; superoxide

615 anion radical).

616 Differences of terms—uncoupled vs. noncoupled—are easily overlooked, although they relate to

617 different meanings of uncoupling (Figure 3 and Table 2).

## 618 2.5. Coupling states and respiratory rates

619

620

621

622

623

624

625

626

627

628

629

630

631

To extend the classical nomenclature on mitochondrial coupling states (Section 2.6) by a concept-driven terminology that explicitly incorporates information on the meaning of respiratory states, the terminology must be general and not restricted to any particular experimental protocol or mitochondrial preparation (Gnaiger 2009). Concept-driven nomenclature aims at mapping the meaning and concept behind the words and acronyms onto the forms of words and acronyms (Miller 1991). The focus of concept-driven nomenclature is primarily the conceptual *why*, along with clarification of the experimental *how*.

**Table 1. Coupling states and residual oxygen consumption in mitochondrial preparations in relation to respiration- and phosphorylation-flux,  $J_{\text{KO}_2}$  and  $J_{\text{P}}$ , and protonmotive force,  $\Delta p$ .** Coupling states are established at kinetically-saturating concentrations of fuel substrates and  $\text{O}_2$ .

State	$J_{\text{KO}_2}$	$J_{\text{P}}$	$\Delta p$	Inducing factors	Limiting factors
LEAK	$L$ ; low, cation leak-dependent respiration	0	max.	back-flux of cations including proton leak, proton slip	$J_{\text{P}} = 0$ : (1) without ADP, $L_{\text{N}}$ ; (2) max. ATP/ADP ratio, $L_{\text{T}}$ ; or (3) inhibition of the phosphorylation-pathway, $L_{\text{Omy}}$
OXPHOS	$P$ ; high, ADP-stimulated respiration, OXPHOS-capacity	max.	high	kinetically-saturating [ADP] and $[\text{P}_i]$	$J_{\text{P}}$ by phosphorylation-pathway; or $J_{\text{KO}_2}$ by ET-capacity
ET	$E$ ; max., noncoupled respiration, ET-capacity	0	low	optimal external uncoupler concentration for max. $J_{\text{O}_2, \text{E}}$	$J_{\text{KO}_2}$ by ET-capacity
ROX	$R_{\text{ox}}$ ; min., residual $\text{O}_2$ consumption	0	0	$J_{\text{O}_2, \text{Rox}}$ in non-ET-pathway oxidation reactions	inhibition of all ET-pathways; or absence of fuel substrates

632

633

634

635

636

637

638

639

640

641

642

643

644

645

646

647

648

649

650

651

652

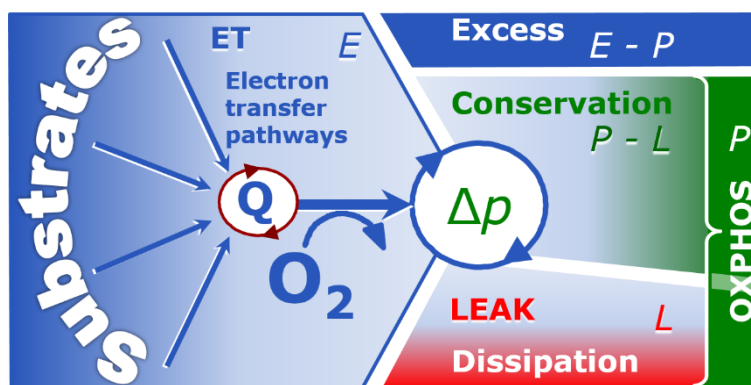
653

To provide a diagnostic reference for respiratory capacities of core energy metabolism, the capacity of oxidative phosphorylation, OXPHOS, is measured at kinetically-saturating concentrations of ADP and  $\text{P}_i$ . The oxidative ET-capacity reveals the limitation of OXPHOS-capacity mediated by the phosphorylation-pathway. The ET- and phosphorylation-pathways comprise coupled segments of the OXPHOS-system. ET-capacity is measured as noncoupled respiration by application of external uncouplers. The contribution of intrinsically uncoupled  $\text{O}_2$  consumption is studied by preventing the stimulation of phosphorylation either in the absence of ADP or by inhibition of the phosphorylation-pathway. The corresponding states are collectively classified as LEAK-states, when  $\text{O}_2$  consumption compensates mainly for ion leaks, including the proton leak. Defined coupling states are induced by: (1) adding cation chelators such as EGTA, binding free  $\text{Ca}^{2+}$  and thus limiting cation cycling; (2) adding ADP and  $\text{P}_i$ ; (3) inhibiting the phosphorylation-pathway; and (4) uncoupler titrations, while maintaining a defined ET-pathway state with constant fuel substrates and inhibitors of specific branches of the ET-pathway.

The three coupling states, ET, LEAK and OXPHOS, are shown schematically with the corresponding respiratory rates, abbreviated as  $E$ ,  $L$  and  $P$ , respectively (**Figure 4**). We distinguish metabolic *pathways* from metabolic *states* and the corresponding metabolic *rates*; for example: ET-pathways, ET-states, and ET-capacities,  $E$ , respectively (**Table 1**). The protonmotive force is *high* in the OXPHOS-state when it drives phosphorylation, *maximum* in the LEAK-state of coupled mitochondria, driven by LEAK-respiration at a minimum back-flux of cations to the matrix side, and *very low* in the ET-state when uncouplers short-circuit the proton cycle (**Table 1**).

654 **Figure 4. Four-compartment**  
655 **model of oxidative**  
656 **phosphorylation**

657 Respiratory states (ET, OXPHOS,  
658 LEAK; Table 1) and corresponding  
659 rates ( $E$ ,  $P$ ,  $L$ ) are connected by the  
660 protonmotive force,  $\Delta p$ . (1) ET-  
661 capacity,  $E$ , is partitioned into (2)  
662 dissipative LEAK-respiration,  $L$ ,  
663 when the Gibbs energy change of  
664 catabolic  $O_2$  flux is irreversibly lost,  
665 (3) net OXPHOS-capacity,  $P-L$ , with  
666 partial conservation of the capacity to  
667 perform work, and (4) the excess capacity,  
 $E-P$ . Modified from Gnaiger (2014).



668 **Figure 5. Respiratory coupling**  
669 **states**

670 **(A) LEAK-state and rate,  $L$ :**

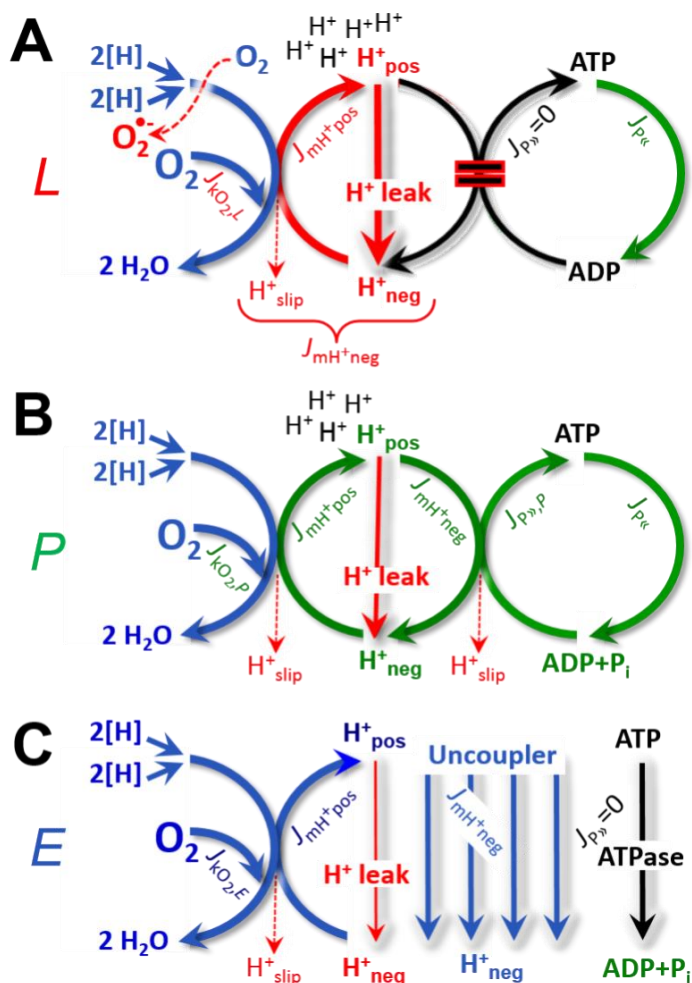
671 Oxidation only, since phosphorylation  
672 is arrested,  $J_{P\gg} = 0$ , and catabolic  $O_2$   
673 flux,  $J_{kO_2,L}$ , is controlled mainly by the  
674 proton leak and slip,  $J_{mH^+neg}$ , at  
675 maximum protonmotive force (Figure  
676 4). Extramitochondrial ATP may be  
677 hydrolyzed by extramitochondrial  
ATPases,  $J_{P\ll}$ ; then phosphorylation  
must be blocked.

678 **(B) OXPHOS-state and rate,  $P$ :**

679 Oxidation coupled to  
680 phosphorylation,  $J_{P\gg}$ , which is  
681 stimulated by kinetically-saturating  
682 [ADP] and  $[P_i]$ , supported by a high  
683 protonmotive force.  $O_2$  flux,  $J_{kO_2,P}$ , is  
684 well-coupled at a  $P\gg/O_2$  ratio of  
685  $J_{P\gg,P}/J_{O_2,P}$ . Extramitochondrial  
686 ATPases may recycle ATP,  $J_{P\ll}$ .

687 **(C) ET-state and rate,  $E$ :**

688 Oxidation only, since phosphorylation is zero,  
689  $J_{P\gg} = 0$ , at optimum exogenous  
690 uncoupler concentration when  
691 noncoupled respiration,  $J_{kO_2,E}$ , is  
692 maximum. The F-ATPase may  
693 hydrolyze extramitochondrial ATP.



668

669 **2.5.1. LEAK-state (Figure 5A):** The LEAK-state is defined as a state of mitochondrial  
670 respiration when  $O_2$  flux mainly compensates for ion leaks in the absence of ATP synthesis,  
671 at kinetically-saturating concentrations of  $O_2$ , respiratory fuel substrates and  $P_i$ . LEAK-respiration is  
672 measured to obtain an estimate of intrinsic uncoupling without addition of an experimental uncoupler:  
673 (1) in the absence of adenylates, *i.e.*, AMP, ADP and ATP; (2) after depletion of ADP at a maximum  
674 ATP/ADP ratio; or (3) after inhibition of the phosphorylation-pathway by inhibitors of F-ATPase—such  
675 as oligomycin, or of adenine nucleotide translocase—such as carboxyatractylsido. Adjustment of the  
676 nominal concentration of these inhibitors to the density of biological sample applied can minimize or  
677 avoid inhibitory side-effects exerted on ET-capacity or even some dyscoupling.

678

**Table 2. Terms on respiratory coupling and uncoupling.**

Term	$J_{kO_2}$	$P \gg O_2$	Notes	
acoupled		0	electron transfer in mitochondrial fragments without vectorial proton translocation ( <b>Figure 3</b> )	
intrinsic, no protonophore added	uncoupled	$L$	0	non-phosphorylating <b>LEAK-respiration</b> ( <b>Figure 5A</b> )
	proton leak-uncoupled		0	component of $L$ , $H^+$ diffusion across the mtIM ( <b>Figure 3</b> )
	decoupled		0	component of $L$ , proton slip ( <b>Figure 3</b> )
	loosely coupled		0	component of $L$ , lower coupling due to superoxide formation and bypass of proton pumps by electron leak ( <b>Figure 3</b> )
	dyscoupled		0	pathologically, toxicologically, environmentally increased uncoupling, mitochondrial dysfunction
	inducibly uncoupled		0	by UCP1 or cation ( <i>e.g.</i> , $Ca^{2+}$ ) cycling ( <b>Figure 3</b> )
noncoupled	$E$	0	ET-capacity, non-phosphorylating respiration stimulated to maximum flux at optimum exogenous uncoupler concentration ( <b>Figure 5C</b> )	
well-coupled	$P$	high	<b>OXPHOS-capacity</b> , phosphorylating respiration with an intrinsic LEAK component ( <b>Figure 5B</b> )	
fully coupled	$P - L$	max.	<b>OXPHOS-capacity</b> corrected for LEAK-respiration ( <b>Figure 4</b> )	

679

680

681

682

683

684

685

686

687

688

689

690

691

692

693

694

695

696

697

698

699

700

701

702

703

704

705

706

- **Proton leak and uncoupled respiration:** The intrinsic proton leak is the *uncoupled* leak current of protons in which protons diffuse across the mtIM in the dissipative direction of the downhill protonmotive force without coupling to phosphorylation (**Figure 5A**). The proton leak flux depends non-linearly on the protonmotive force (Garlid *et al.* 1989; Divakaruni and Brand 2011), which is a temperature-dependent property of the mtIM and may be enhanced due to possible contaminations by free fatty acids. Inducible uncoupling mediated by uncoupling protein 1 (UCP1) is physiologically controlled, *e.g.*, in brown adipose tissue. UCP1 is a member of the mitochondrial carrier family that is involved in the translocation of protons across the mtIM (Klingenberg 2017). Consequently, this short-circuit lowers the protonmotive force and stimulates electron transfer, respiration, and heat dissipation in the absence of phosphorylation of ADP.
- **Cation cycling:** There can be other cation contributors to leak current including calcium and probably magnesium. Calcium influx is balanced by mitochondrial  $Na^+/Ca^{2+}$  or  $H^+/Ca^{2+}$  exchange, which is balanced by  $Na^+/H^+$  or  $K^+/H^+$  exchanges. This is another effective uncoupling mechanism different from proton leak (**Table 2**).
- **Proton slip and decoupled respiration:** Proton slip is the *decoupled* process in which protons are only partially translocated by a redox proton pump of the ET-pathways and slip back to the original vesicular compartment. The proton leak is the dominant contributor to the overall leak current in mammalian mitochondria incubated under physiological conditions at 37 °C, whereas proton slip increases at lower experimental temperature (Canton *et al.* 1995). Proton slip can also happen in association with the F-ATPase, in which the proton slips downhill across the pump to the matrix without contributing to ATP synthesis. In each case, proton slip is a property of the proton pump and increases with the pump turnover rate.
- **Electron leak and loosely coupled respiration:** Superoxide production by the ETS leads to a bypass of redox proton pumps and correspondingly lower  $P \gg O_2$  ratio. This depends on the actual site of electron leak and the scavenging of hydrogen peroxide by cytochrome *c*, whereby electrons may re-enter the ETS with proton translocation by CIV.



- **Loss of compartmental integrity and acoupled respiration:** Electron transfer and catabolic O<sub>2</sub> flux proceed without compartmental proton translocation in disrupted mitochondrial fragments. Such fragments are an artefact of mitochondrial isolation, and may not fully fuse to re-establish structurally intact mitochondria. Loss of mtIM integrity, therefore, is the cause of acoupled respiration, which is a nonvectorial dissipative process without control by the protonmotive force.
- **Dyscoupled respiration:** Mitochondrial injuries may lead to *dyscoupling* as a pathological or toxicological cause of *uncoupled* respiration. Dyscoupling may involve any type of uncoupling mechanism, *e.g.*, opening the permeability transition pore. Dyscoupled respiration is distinguished from the experimentally induced *noncoupled* respiration in the ET-state (**Table 2**).

**2.5.2. OXPHOS-state (Figure 5B):** The OXPHOS-state is defined as the respiratory state with kinetically-saturating concentrations of O<sub>2</sub>, respiratory and phosphorylation substrates, and absence of exogenous uncoupler, which provides an estimate of the maximal respiratory capacity in the OXPHOS-state for any given ET-pathway state. Respiratory capacities at kinetically-saturating substrate concentrations provide reference values or upper limits of performance, aiming at the generation of data sets for comparative purposes. Physiological activities and effects of substrate kinetics can be evaluated relative to the OXPHOS-capacity.

As discussed previously, 0.2 mM ADP does not fully saturate flux in isolated mitochondria (Gnaiger 2001; Puchowicz *et al.* 2004); greater [ADP] is required, particularly in permeabilized muscle fibres and cardiomyocytes, to overcome limitations by intracellular diffusion and by the reduced conductance of the mtOM (Jepihhina *et al.* 2011, Illaste *et al.* 2012, Simson *et al.* 2016), either through interaction with tubulin (Rostovtseva *et al.* 2008) or other intracellular structures (Birkedal *et al.* 2014). In addition, saturating ADP concentrations need to be evaluated under different experimental conditions such as temperature (Lemieux *et al.* 2017) and with different animal models (Blier and Guderley, 1993). In permeabilized muscle fibre bundles of high respiratory capacity, the apparent  $K_m$  for ADP increases up to 0.5 mM (Saks *et al.* 1998), consistent with experimental evidence that >90% saturation is reached only at >5 mM ADP (Pesta and Gnaiger 2012). Similar ADP concentrations are also required for accurate determination of OXPHOS-capacity in human clinical cancer samples and permeabilized cells (Klepinin *et al.* 2016; Koit *et al.* 2017). Whereas 2.5 to 5 mM ADP is sufficient to obtain the actual OXPHOS-capacity in many types of permeabilized tissue and cell preparations, experimental validation is required in each specific case.

**2.5.3. Electron transfer-state (Figure 5C):** O<sub>2</sub> flux determined in the ET-state yields an estimate of ET-capacity. The ET-state is defined as the *noncoupled* state with kinetically-saturating concentrations of O<sub>2</sub>, respiratory substrate and optimum exogenous uncoupler concentration for maximum O<sub>2</sub> flux. Uncouplers are weak lipid-soluble acids which function as protonophores. These disrupt the barrier function of the mtIM and thus short circuit the protonmotive system, functioning like a clutch in a mechanical system. As a consequence of the nearly collapsed protonmotive force, the driving force is insufficient for phosphorylation, and  $J_{P_s} = 0$ . The most frequently used uncouplers are carbonyl cyanide *m*-chloro phenyl hydrazone (CCCP), carbonyl cyanide *p*-trifluoromethoxyphenylhydrazone (FCCP), or dinitrophenole (DNP). Stepwise titration of uncouplers stimulates respiration up to or above the level of O<sub>2</sub> consumption rates in the OXPHOS-state; respiration is inhibited, however, above optimum uncoupler concentrations (Mitchell 2011). Data obtained with a single dose of uncoupler must be evaluated with caution, particularly when a fixed uncoupler concentration is used in studies exploring a treatment or disease that may alter the mitochondrial content or mitochondrial sensitivity to inhibition by uncouplers. The effect on ET-capacity of the reversed function of F-ATPase ( $J_{P_r}$ ; **Figure 5C**) can be evaluated in the presence and absence of extramitochondrial ATP.

**2.5.4. ROX state and *Rox*:** Besides the three fundamental coupling states of mitochondrial preparations, the state of residual O<sub>2</sub> consumption, ROX, is relevant to assess respiratory function (**Figure 1**). ROX is not a coupling state. The rate of residual oxygen consumption, *Rox*, is defined as O<sub>2</sub> consumption due to oxidative reactions measured after inhibition of ET—with rotenone, malonic acid and antimycin A. Cyanide and azide inhibit not only CIV but catalase and several peroxidases involved in *Rox*. High concentrations of antimycin A, but not rotenone or cyanide, inhibit peroxisomal acyl-CoA oxidase and D-amino acid oxidase (Vamecq *et al.* 1987). *Rox* represents a baseline that is used to correct respiration measured in defined coupling states. *Rox*-corrected *L*, *P* and *E* not only lower the values of total fluxes, but also change the flux control ratios *L/P* and *L/E*. *Rox* is not necessarily equivalent to non-

763 mitochondrial reduction of O<sub>2</sub>, considering O<sub>2</sub>-consuming reactions in mitochondria that are not related  
 764 to ET—such as O<sub>2</sub> consumption in reactions catalyzed by monoamine oxidases (type A and B),  
 765 monoxygenases (cytochrome P450 monoxygenases), dioxygenase (sulfur dioxygenase and  
 766 trimethyllysine dioxygenase), and several hydroxylases. Even isolated mitochondrial fractions,  
 767 especially those obtained from liver, may be contaminated by peroxisomes. This fact makes the exact  
 768 determination of mitochondrial O<sub>2</sub> consumption and mitochondria-associated generation of reactive  
 769 oxygen species complicated (Schönfeld *et al.* 2009; Speijer 2016; **Figure 2**). The dependence of ROX-  
 770 linked O<sub>2</sub> consumption needs to be studied in detail together with non-ET enzyme activities, availability  
 771 of specific substrates, O<sub>2</sub> concentration, and electron leakage leading to the formation of reactive oxygen  
 772 species.

773 **2.5.5. Quantitative relations:**  $E$  may exceed or be equal to  $P$ .  $E > P$  is observed in many types  
 774 of mitochondria, varying between species, tissues and cell types (Gnaiger 2009).  $E - P$  is the excess ET-  
 775 capacity pushing the phosphorylation-flux (**Figure 2C**) to the limit of its capacity of utilizing the  
 776 protonmotive force. In addition, the magnitude of  $E - P$  depends on the tightness of respiratory coupling  
 777 or degree of uncoupling, since an increase of  $L$  causes  $P$  to increase towards the limit of  $E$ . The *excess*  
 778  $E - P$  capacity,  $E - P$ , therefore, provides a sensitive diagnostic indicator of specific injuries of the  
 779 phosphorylation-pathway, under conditions when  $E$  remains constant but  $P$  declines relative to controls  
 780 (**Figure 4**). Substrate cocktails supporting simultaneous convergent electron transfer to the Q-junction  
 781 for reconstitution of TCA cycle function establish pathway control states with high ET-capacity, and  
 782 consequently increase the sensitivity of the  $E - P$  assay.

783  $E$  cannot theoretically be lower than  $P$ .  $E < P$  must be discounted as an artefact, which may be  
 784 caused experimentally by: (1) loss of oxidative capacity during the time course of the respirometric  
 785 assay, since  $E$  is measured subsequently to  $P$ ; (2) using insufficient uncoupler concentrations; (3) using  
 786 high uncoupler concentrations which inhibit ET (Gnaiger 2008); (4) high oligomycin concentrations  
 787 applied for measurement of  $L$  before titrations of uncoupler, when oligomycin exerts an inhibitory effect  
 788 on  $E$ . On the other hand, the excess ET-capacity is overestimated if non-saturating [ADP] or [P<sub>i</sub>] are  
 789 used. See State 3 in the next section.

790 The net OXPHOS-capacity is calculated by subtracting  $L$  from  $P$  (**Figure 4**). The net P»/O<sub>2</sub> equals  
 791 P»/( $P - L$ ), wherein the dissipative LEAK component in the OXPHOS-state may be overestimated. This  
 792 can be avoided by measuring LEAK-respiration in a state when the protonmotive force is adjusted to its  
 793 slightly lower value in the OXPHOS-state—by titration of an ET inhibitor (Divakaruni and Brand 2011).  
 794 Any turnover-dependent components of proton leak and slip, however, are underestimated under these  
 795 conditions (Garlid *et al.* 1993). In general, it is inappropriate to use the term *ATP production* or *ATP*  
 796 *turnover* for the difference of O<sub>2</sub> flux measured in the OXPHOS and LEAK states.  $P - L$  is the upper limit  
 797 of OXPHOS-capacity that is freely available for ATP production (corrected for LEAK-respiration) and  
 798 is fully coupled to phosphorylation with a maximum mechanistic stoichiometry (**Figure 4**).

799 The rates of LEAK respiration and OXPHOS capacity depend on (1) the tightness of coupling  
 800 under the influence of the respiratory uncoupling mechanisms (**Figure 3**), and (2) the coupling  
 801 stoichiometry, which varies as a function of the substrate type undergoing oxidation in ET-pathways  
 802 with either two or three coupling sites (**Figure 2B**). When cocktails with NADH-linked substrates and  
 803 succinate are used, the relative contribution of ET-pathways with three or two coupling sites cannot be  
 804 controlled experimentally, is difficult to determine, and may shift in transitions between LEAK-,  
 805 OXPHOS- and ET-states (Gnaiger 2014). Under these experimental conditions, we cannot separate the  
 806 tightness of coupling *versus* coupling stoichiometry as the mechanisms of respiratory control in the shift  
 807 of  $L/P$  ratios. The tightness of coupling and fully coupled O<sub>2</sub> flux,  $P - L$  (**Table 2**), therefore, are obtained  
 808 from measurements of coupling control of LEAK respiration, OXPHOS- and ET-capacities in well  
 809 defined pathway states, using either pyruvate and malate as substrates or the classical succinate and  
 810 rotenone substrate-inhibitor combination (**Figure 2B**).

811 **2.5.6. The steady-state:** Mitochondria represent a thermodynamically open system in non-  
 812 equilibrium states of biochemical energy transformation. State variables (protonmotive force; redox  
 813 states) and metabolic *rates* (fluxes) are measured in defined mitochondrial respiratory *states*. Steady-  
 814 states can be obtained only in open systems, in which changes by internal transformations, *e.g.*, O<sub>2</sub>  
 815 consumption, are instantaneously compensated for by external fluxes, *e.g.*, O<sub>2</sub> supply, preventing a  
 816 change of O<sub>2</sub> concentration in the system (Gnaiger 1993b). Mitochondrial respiratory states monitored  
 817 in closed systems satisfy the criteria of pseudo-steady states for limited periods of time, when changes  
 818 in the system (concentrations of O<sub>2</sub>, fuel substrates, ADP, P<sub>i</sub>, H<sup>+</sup>) do not exert significant effects on

819 metabolic fluxes (respiration, phosphorylation). Such pseudo-steady states require respiratory media  
 820 with sufficient buffering capacity and substrates maintained at kinetically-saturating concentrations, and  
 821 thus depend on the kinetics of the processes under investigation.

822  
 823 **2.6. Classical terminology for isolated mitochondria**

824 'When a code is familiar enough, it ceases appearing like a code; one forgets that there is a  
 825 decoding mechanism. The message is identical with its meaning' (Hofstadter 1979).

826  
 827 Chance and Williams (1955; 1956) introduced five classical states of mitochondrial respiration  
 828 and cytochrome redox states. **Table 3** shows a protocol with isolated mitochondria in a closed  
 829 respirometric chamber, defining a sequence of respiratory states. States and rates are not specifically  
 830 distinguished in this nomenclature.

831  
 832  
 833  
 834

**Table 3. Metabolic states of mitochondria (Chance and Williams, 1956; Table V).**

State	[O <sub>2</sub> ]	ADP level	Substrate level	Respiration rate	Rate-limiting substance
1	>0	low	low	slow	ADP
2	>0	high	~0	slow	substrate
3	>0	high	high	fast	respiratory chain
4	>0	low	high	slow	ADP
5	0	high	high	0	oxygen

835  
 836

837 **2.6.1. State 1** is obtained after addition of isolated mitochondria to air-saturated  
 838 isoosmotic/isotonic respiration medium containing P<sub>i</sub>, but no fuel substrates and no adenylates, *i.e.*,  
 839 AMP, ADP, ATP.

840 **2.6.2. State 2** is induced by addition of a 'high' concentration of ADP (typically 100 to 300 μM),  
 841 which stimulates respiration transiently on the basis of endogenous fuel substrates and phosphorylates  
 842 only a small portion of the added ADP. State 2 is then obtained at a low respiratory activity limited by  
 843 exhausted endogenous fuel substrate availability (**Table 3**). If addition of specific inhibitors of  
 844 respiratory complexes—such as rotenone—does not cause a further decline of O<sub>2</sub> flux, State 2 is  
 845 equivalent to the ROX state (See below.). If inhibition is observed, undefined endogenous fuel substrates  
 846 are a confounding factor of pathway control, contributing to the effect of subsequently externally added  
 847 substrates and inhibitors. In contrast to the original protocol, an alternative sequence of titration steps is  
 848 frequently applied, in which the alternative 'State 2' has an entirely different meaning, when this second  
 849 state is induced by addition of fuel substrate without ADP or ATP (LEAK-state; in contrast to State 2  
 850 defined in **Table 1** as a ROX state). Some researchers have called this condition as "pseudostate 4"  
 851 because it has no significant concentrations of adenine nucleotides and hence it is not a near-  
 852 physiological condition, although it should be used for calculating the net OXPHOS-capacity, *P-L*.

853 **2.6.3. State 3** is the state stimulated by addition of fuel substrates while the ADP concentration  
 854 is still high (**Table 3**) and supports coupled energy transformation through oxidative phosphorylation.  
 855 'High ADP' is a concentration of ADP specifically selected to allow the measurement of State 3 to State  
 856 4 transitions of isolated mitochondria in a closed respirometric chamber. Repeated ADP titration re-  
 857 establishes State 3 at 'high ADP'. Starting at O<sub>2</sub> concentrations near air-saturation (193 or 238 μM O<sub>2</sub>  
 858 at 37 °C or 25 °C and sea level at 1 atm or 101.32 kPa, and an oxygen solubility of respiration medium  
 859 at 0.92 times that of pure water; Forstner and Gnaiger 1983), the total ADP concentration added must  
 860 be low enough (typically 100 to 300 μM) to allow phosphorylation to ATP at a coupled O<sub>2</sub> flux that  
 861 does not lead to O<sub>2</sub> depletion during the transition to State 4. In contrast, kinetically-saturating ADP  
 862 concentrations usually are 10-fold higher than 'high ADP', *e.g.*, 2.5 mM in isolated mitochondria. The  
 863 abbreviation State 3u is occasionally used in bioenergetics, to indicate the state of respiration after  
 864 titration of an uncoupler, without sufficient emphasis on the fundamental difference between OXPHOS-  
 865 capacity (*well-coupled* with an endogenous uncoupled component) and ET-capacity (*noncoupled*).

866 **2.6.4. State 4** is a LEAK-state that is obtained only if the mitochondrial preparation is intact and  
 867 well-coupled. Depletion of ADP by phosphorylation to ATP causes a decline of O<sub>2</sub> flux in the transition  
 868 from State 3 to State 4. Under the conditions of State 4, a maximum protonmotive force and high  
 869 ATP/ADP ratio are maintained. The gradual decline of  $Y_{P\gg/O_2}$  towards diminishing [ADP] at State 4 must  
 870 be taken into account for calculation of  $P\gg/O_2$  ratios (Gnaiger 2001). State 4 respiration,  $L_T$  (**Table 1**),  
 871 reflects intrinsic proton leak and ATP hydrolysis activity. O<sub>2</sub> flux in State 4 is an overestimation of  
 872 LEAK-respiration if the contaminating ATP hydrolysis activity recycles some ATP to ADP,  $J_{P\ll}$ , which  
 873 stimulates respiration coupled to phosphorylation,  $J_{P\gg} > 0$ . Some degree of mechanical disruption and  
 874 loss of mitochondrial integrity allows the exposed mitochondrial F-ATPases to hydrolyze the ATP  
 875 synthesized by the fraction of coupled mitochondria. This can be tested by inhibition of the  
 876 phosphorylation-pathway using oligomycin, ensuring that  $J_{P\gg} = 0$  (State 4o). On the other hand, the State  
 877 4 respiration reached after exhaustion of added ADP is a more physiological condition (*i.e.*, presence of  
 878 ATP, ADP and even AMP). Sequential ADP titrations re-establish State 3, followed by State 3 to State  
 879 4 transitions while sufficient O<sub>2</sub> is available. Anoxia may be reached, however, before exhaustion of  
 880 ADP (State 5).

881 **2.6.5. State 5** is the state after exhaustion of O<sub>2</sub> in a closed respirometric chamber. Diffusion of  
 882 O<sub>2</sub> from the surroundings into the aqueous solution may be a confounding factor preventing complete  
 883 anoxia (Gnaiger 2001). Chance and Williams (1955) provide an alternative definition of State 5, which  
 884 gives it the different meaning of ROX versus anoxia: ‘State 5 may be obtained by antimycin A treatment  
 885 or by anaerobiosis’.

886 In **Table 3**, only States 3 and 4 are coupling control states, with the restriction that rates in State  
 887 3 may be limited kinetically by non-saturating ADP concentrations.

## 888 2.7. Control and regulation

891 The terms metabolic *control* and *regulation* are frequently used synonymously, but are  
 892 distinguished in metabolic control analysis: ‘We could understand the regulation as the mechanism that  
 893 occurs when a system maintains some variable constant over time, in spite of fluctuations in external  
 894 conditions (homeostasis of the internal state). On the other hand, metabolic control is the power to  
 895 change the state of the metabolism in response to an external signal’ (Fell 1997). Respiratory control  
 896 may be induced by experimental control signals that exert an influence on: (1) ATP demand and ADP  
 897 phosphorylation-rate; (2) fuel substrate composition, pathway competition; (3) available amounts of  
 898 substrates and O<sub>2</sub>, *e.g.*, starvation and hypoxia; (4) the protonmotive force, redox states, flux–force  
 899 relationships, coupling and efficiency; (5) Ca<sup>2+</sup> and other ions including H<sup>+</sup>; (6) inhibitors, *e.g.*, nitric  
 900 oxide or intermediary metabolites such as oxaloacetate; (7) signalling pathways and regulatory proteins,  
 901 *e.g.*, insulin resistance, transcription factor hypoxia inducible factor 1.

902 Mechanisms of respiratory control and regulation include adjustments of: (1) enzyme activities  
 903 by allosteric mechanisms and phosphorylation; (2) enzyme content, concentrations of cofactors and  
 904 conserved moieties—such as adenylates, nicotinamide adenine dinucleotide [NAD<sup>+</sup>/NADH], coenzyme  
 905 Q, cytochrome *c*; (3) metabolic channeling by supercomplexes; and (4) mitochondrial density (enzyme  
 906 concentrations and membrane area) and morphology (cristae folding, fission and fusion). Mitochondria  
 907 are targeted directly by hormones, *e.g.*, progesterone and glucacorticoids, which affect their energy  
 908 metabolism (Lee *et al.* 2013; Gerö and Szabo 2016; Price and Dai 2016; Moreno *et al.* 2017).  
 909 Evolutionary or acquired differences in the genetic and epigenetic basis of mitochondrial function (or  
 910 dysfunction) between individuals; age; biological sex, and hormone concentrations; life style including  
 911 exercise and nutrition; and environmental issues including thermal, atmospheric, toxic and  
 912 pharmacological factors, exert an influence on all control mechanisms listed above. For reviews, see  
 913 Brown 1992; Gnaiger 1993a, 2009; 2014; Paradies *et al.* 2014; Morrow *et al.* 2017.

914 Lack of control by a metabolic pathway, *e.g.*, phosphorylation-pathway, means that there will  
 915 be no response to a variable activating it, *e.g.*, [ADP]. The reverse, however, is not true as the absence  
 916 of a response to [ADP] does not exclude the phosphorylation-pathway from having some degree of  
 917 control. The degree of control of a component of the OXPHOS-pathway on an output variable—such  
 918 as O<sub>2</sub> flux, will in general be different from the degree of control on other outputs—such as  
 919 phosphorylation-flux or proton leak flux. Therefore, it is necessary to be specific as to which input and  
 920 output are under consideration (Fell 1997).

921 Respiratory control refers to the ability of mitochondria to adjust  $O_2$  flux in response to external  
 922 control signals by engaging various mechanisms of control and regulation. Respiratory control is  
 923 monitored in a mitochondrial preparation under conditions defined as respiratory states, preferentially  
 924 under near-physiological conditions of temperature, pH and medium ionic composition, to generate data  
 925 of higher biological relevance. When phosphorylation of ADP to ATP is stimulated or depressed, an  
 926 increase or decrease is observed in electron transfer measured as  $O_2$  flux in respiratory coupling states  
 927 of intact mitochondria ('controlled states' in the classical terminology of bioenergetics). Alternatively,  
 928 coupling of electron transfer with phosphorylation is diminished by uncouplers. The corresponding  
 929 coupling control state is characterized by a high respiratory rate without control by P» (noncoupled or  
 930 'uncontrolled state').

931  
 932

### 933 3. What is a rate?

934

935 The term *rate* is not adequately defined to be useful for reporting data. Normalization of 'rates'  
 936 leads to a diversity of formats. Application of common and defined units is required for direct transfer  
 937 of reported results into a database. The second [s] is the SI unit for the base quantity *time*. It is also the  
 938 standard time-unit used in solution chemical kinetics.

939 The inconsistency of the meanings of rate becomes apparent when considering Galileo Galilei's  
 940 famous principle, that 'bodies of different weight all fall at the same rate (have a constant acceleration)'  
 941 (Coopersmith 2010). A rate may be an extensive quantity, which is a *flow*,  $I$ , when expressed per object  
 942 (per number of cells or organisms) or per chamber (per system). 'System' is defined as the open or  
 943 closed chamber of the measuring device. A rate is a *flux*,  $J$ , when expressed as a size-specific quantity  
 944 (Figure 6A; Box 2).

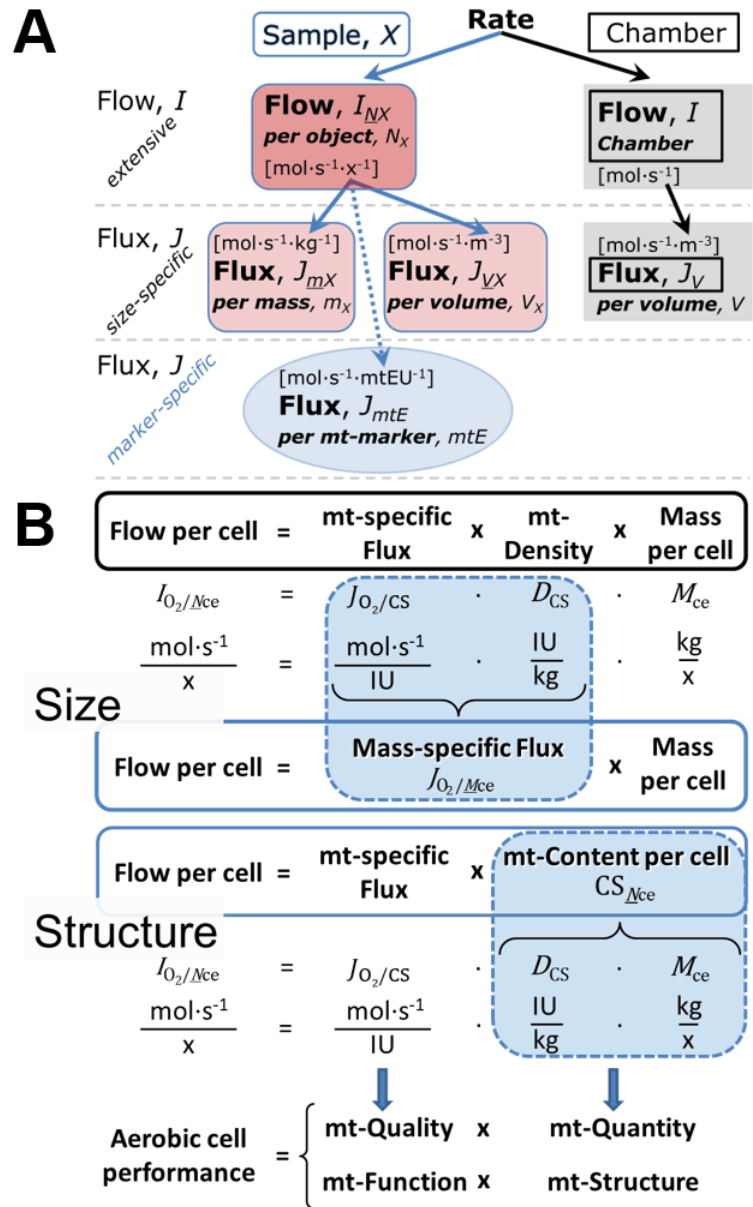
- 945 • **Extensive quantities:** An extensive quantity increases proportionally with system size. For  
 946 example, mass and volume are extensive quantities. Flow is an extensive quantity. The  
 947 magnitude of an extensive quantity is completely additive for non-interacting subsystems.  
 948 The magnitude of these quantities depends on the extent or size of the system (Cohen *et al.*  
 949 2008).
- 950 • **Size-specific quantities:** 'The adjective *specific* before the name of an extensive quantity is  
 951 often used to mean *divided by mass*' (Cohen *et al.* 2008). In this system-paradigm, mass-  
 952 specific flux is flow divided by mass of the system (the total mass of everything within the  
 953 measuring chamber or reactor). Rates are frequently expressed as volume-specific flux. A  
 954 mass-specific or volume-specific quantity is independent of the extent of non-interacting  
 955 homogenous subsystems. Tissue-specific quantities (related to the *sample* in contrast to the  
 956 *system*) are of fundamental interest in the field of comparative mitochondrial physiology,  
 957 where *specific* refers to the *type of the sample* rather than *mass of the system*. The term  
 958 *specific*, therefore, must be clarified; *sample-specific*, *e.g.*, muscle mass-specific  
 959 normalization, is distinguished from *system-specific* quantities (mass or volume; Figure 6).
- 960 • **Intensive quantities:** In contrast to size-specific properties, forces are intensive quantities  
 961 defined as the change of an extensive quantity per advancement of an energy transformation  
 962 (Gnaiger 1993b).
- 963 •  $N_X$  and  $m_X$  indicate the number format and mass format, respectively, for expressing the  
 964 quantity of a sample  $X$ . When different formats are indicated in symbols of derived quantities,  
 965 the format ( $\underline{N}$ ,  $\underline{m}$ ) is shown as a subscript (*underlined italic*), as in  $I_{O_2/\underline{N}X}$  and  $J_{O_2/\underline{m}X}$ . Oxygen  
 966 flow and flux are expressed in the molar format,  $n_{O_2}$  [mol], but in the volume format,  $V_{O_2}$  [m<sup>3</sup>]  
 967 in ergometry. For mass-specific flux these formats can be distinguished as  $J_{nO_2/\underline{m}X}$  and  $J_{VO_2/\underline{m}X}$ ,  
 968 respectively. Further examples are given in Figure 6 and Table 4.

969

970 **Figure 6. Flow and flux, and**  
 971 **normalization in structure-**  
 972 **function analysis**

973 (A) When expressing metabolic  
 974 ‘rate’ measured in a chamber, a  
 975 fundamental distinction is made  
 976 between relating the rate to the  
 977 experimental sample (left) or  
 978 chamber (right). The different  
 979 meanings of rate need to be  
 980 specified by the chosen  
 981 normalization. Left: Results are  
 982 expressed as mass-specific flux,  $J_{mX}$ ,  
 983 per mg protein, dry or wet mass.  
 984 Cell volume,  $V_{ce}$ , may be used for  
 985 normalization (volume-specific  
 986 flux,  $J_{Vce}$ ). Right: Flow per chamber,  
 987  $I$ , or flux per chamber volume,  $J_V$ ,  
 988 are merely reported for  
 989 methodological reasons.

990 (B)  $O_2$  flow per cell,  $I_{O_2/Nce}$ , is the  
 991 product of mitochondria-specific  
 992 flux, mt-density and mass per cell.  
 993 Unstructured analysis: performance  
 994 is the product of mass-specific flux,  
 995  $J_{O_2/MX}$  [ $\text{mol}\cdot\text{s}^{-1}\cdot\text{kg}^{-1}$ ], and size  
 996 (mass per cell). Structured analysis:  
 997 performance is the product of  
 998 mitochondrial function (mt-specific  
 999 flux) and structure (mt-content).  
 1000 Modified from Gnaiger (2014). For  
 1001 further details see **Table 4**.



1007 **Box 2: Metabolic flows and fluxes: vectoral, vectorial, and scalar**

1008  
 1009 In a generalization of electrical terms, flow as an extensive quantity ( $I$ ; per system) is  
 1010 distinguished from flux as a size-specific quantity ( $J$ ; per system size). *Flows*,  $I_{tr}$ , are defined for all  
 1011 transformations as extensive quantities. Electric charge per unit time is electric flow or current,  $I_{el} =$   
 1012  $dQ_{el} \cdot dt^{-1}$  [ $A \equiv C \cdot s^{-1}$ ]. When dividing  $I_{el}$  by size of the system (cross-sectional area of a ‘wire’), we obtain  
 1013 flux as a size-specific quantity, which is the current density (surface-density of flow) perpendicular to  
 1014 the direction of flux,  $J_{el} = I_{el} \cdot A^{-1}$  [ $A \cdot m^{-2}$ ] (Cohen et al. 2008). Fluxes with *spatial* geometric direction and  
 1015 magnitude are *vectors*. Vector and scalar *fluxes* are related to flows as  $J_{tr} = I_{tr} \cdot A^{-1}$  [ $\text{mol}\cdot\text{s}^{-1}\cdot\text{m}^{-2}$ ] and  $J_{tr} =$   
 1016  $I_{tr} \cdot V^{-1}$  [ $\text{mol}\cdot\text{s}^{-1}\cdot\text{m}^{-3}$ ], expressing flux as an area-specific vector or volume-specific vectorial or scalar  
 1017 quantity, respectively (Gnaiger 1993b). We use the metre–kilogram–second–ampere (MKSA)  
 1018 international system of units (SI) for general cases ([m], [kg], [s] and [A]), with decimal SI prefixes for  
 1019 specific applications (**Table 4**).

1020 We suggest to define: (1) *vectoral* fluxes, which are translocations as functions of *gradients* with  
 1021 direction in geometric space in continuous systems; (2) *vectorial* fluxes, which describe translocations  
 1022 in discontinuous systems and are restricted to information on *compartmental differences*  
 1023 (transmembrane proton flux); and (3) *scalar* fluxes, which are transformations in a *homogenous* system  
 1024 (catabolic  $O_2$  flux,  $J_{kO_2}$ ).

#### 4. Normalization of rate per sample

The challenges of measuring mitochondrial respiratory flux are matched by those of normalization. Normalization (**Table 4**) is guided by physicochemical principles, methodological considerations, and conceptual strategies (**Figure 6**).

**Table 4. Sample concentrations and normalization of flux.**

Expression	Symbol	Definition	Unit	Notes
<b>Sample</b>				
identity of sample	$X$	object: cell, tissue, animal, patient		
number of sample entities $X$	$N_X$	number of objects	x	1
mass of sample $X$	$m_X$		kg	2
mass of object $X$	$M_X$	$M_X = m_X \cdot N_X^{-1}$	$\text{kg} \cdot \text{x}^{-1}$	2
<b>Mitochondria</b>				
mitochondria	mt	$X = \text{mt}$		
amount of mt-elementary components	$mtE$	quantity of mt-marker	mtEU	
<b>Concentrations</b>				
object number concentration	$C_{NX}$	$C_{NX} = N_X \cdot V^{-1}$	$\text{x} \cdot \text{m}^{-3}$	3
sample mass concentration	$C_{mX}$	$C_{mX} = m_X \cdot V^{-1}$	$\text{kg} \cdot \text{m}^{-3}$	
mitochondrial concentration	$C_{mtE}$	$C_{mtE} = mtE \cdot V^{-1}$	$\text{mtEU} \cdot \text{m}^{-3}$	4
specific mitochondrial density	$D_{mtE}$	$D_{mtE} = mtE \cdot m_X^{-1}$	$\text{mtEU} \cdot \text{kg}^{-1}$	5
mitochondrial content, $mtE$ per object $X$	$mtE_{NX}$	$mtE_{NX} = mtE \cdot N_X^{-1}$	$\text{mtEU} \cdot \text{x}^{-1}$	6
<b>O<sub>2</sub> flow and flux</b>				
flow, system	$I_{O_2}$	internal flow	$\text{mol} \cdot \text{s}^{-1}$	8
volume-specific flux	$J_{V,O_2}$	$J_{V,O_2} = I_{O_2} \cdot V^{-1}$	$\text{mol} \cdot \text{s}^{-1} \cdot \text{m}^{-3}$	9
flow per object $X$	$I_{O_2/NX}$	$I_{O_2/NX} = J_{V,O_2} \cdot C_{NX}^{-1}$	$\text{mol} \cdot \text{s}^{-1} \cdot \text{x}^{-1}$	10
mass-specific flux	$J_{O_2/mX}$	$J_{O_2/mX} = J_{V,O_2} \cdot C_{mX}^{-1}$	$\text{mol} \cdot \text{s}^{-1} \cdot \text{kg}^{-1}$	
mt-marker-specific flux	$J_{O_2/mtE}$	$J_{O_2/mtE} = J_{V,O_2} \cdot C_{mtE}^{-1}$	$\text{mol} \cdot \text{s}^{-1} \cdot \text{mtEU}^{-1}$	11

- 1033 1 The unit x for a number is not used by IUPAC. To avoid confusion, the units [ $\text{kg} \cdot \text{x}^{-1}$ ] and [kg] distinguish the mass per object from the mass of a sample that may contain any number of objects. Similarly, the units for flow per system *versus* flow per object are [ $\text{mol} \cdot \text{s}^{-1}$ ] (Note 8) and [ $\text{mol} \cdot \text{s}^{-1} \cdot \text{x}^{-1}$ ] (Note 10).
- 1034 2 Units are given in the MKSA system (**Box 2**). The *SI* prefix k is used for the *SI* base unit of mass (kg = 1,000 g). In praxis, various *SI* prefixes are used for convenience, to make numbers easily readable, e.g., 1 mg tissue, cell or mitochondrial mass instead of 0.000001 kg.
- 1035 3 In case of cells (sample  $X = \text{cells}$ ), the object number concentration is  $C_{N_{ce}} = N_{ce} \cdot V^{-1}$ , and volume may be expressed in [ $\text{dm}^3 \equiv \text{L}$ ] or [ $\text{cm}^3 = \text{mL}$ ]. See **Table 5** for different object types.
- 1036 4 mt-concentration is an experimental variable, dependent on sample concentration: (1)  $C_{mtE} = mtE \cdot V^{-1}$ ; (2)  $C_{mtE} = mtE_X \cdot C_{NX}$ ; (3)  $C_{mtE} = C_{mX} \cdot D_{mtE}$ .
- 1037 5 If the amount of mitochondria,  $mtE$ , is expressed as mitochondrial mass, then  $D_{mtE}$  is the mass fraction of mitochondria in the sample. If  $mtE$  is expressed as mitochondrial volume,  $V_{mt}$ , and the mass of sample,  $m_X$ , is replaced by volume of sample,  $V_X$ , then  $D_{mtE}$  is the volume fraction of mitochondria in the sample.
- 1038 6  $mtE_{NX} = mtE \cdot N_X^{-1} = C_{mtE} \cdot C_{NX}^{-1}$ .
- 1039 7 O<sub>2</sub> can be replaced by other chemicals to study different reactions, e.g., ATP, H<sub>2</sub>O<sub>2</sub>, or vesicular compartmental translocations, e.g., Ca<sup>2+</sup>.
- 1040
- 1041
- 1042
- 1043
- 1044
- 1045
- 1046
- 1047
- 1048
- 1049
- 1050

- 1051 8  $I_{O_2}$  and  $V$  are defined per instrument chamber as a system of constant volume (and constant  
 1052 temperature), which may be closed or open.  $I_{O_2}$  is abbreviated for  $I_{rO_2}$ , *i.e.*, the metabolic or internal  
 1053  $O_2$  flow of the chemical reaction  $r$  in which  $O_2$  is consumed, hence the negative stoichiometric  
 1054 number,  $\nu_{O_2} = -1$ .  $I_{rO_2} = d_r n_{O_2} / dt \cdot \nu_{O_2}^{-1}$ . If  $r$  includes all chemical reactions in which  $O_2$  participates, then  
 1055  $d_r n_{O_2} = dn_{O_2} - d_e n_{O_2}$ , where  $dn_{O_2}$  is the change in the amount of  $O_2$  in the instrument chamber and  $d_e n_{O_2}$   
 1056 is the amount of  $O_2$  added externally to the system. At steady state, by definition  $dn_{O_2} = 0$ , hence  $d_r n_{O_2}$   
 1057  $= -d_e n_{O_2}$ .
- 1058 9  $J_{V,O_2}$  is an experimental variable, expressed per volume of the instrument chamber.
- 1059 10  $I_{O_2/NX}$  is a physiological variable, depending on the size of entity  $X$ .
- 1060 11 There are many ways to normalize for a mitochondrial marker, that are used in different experimental  
 1061 approaches: (1)  $J_{O_2/mtE} = J_{V,O_2} \cdot C_{mtE}^{-1}$ ; (2)  $J_{O_2/mtE} = J_{V,O_2} \cdot C_{mX}^{-1} \cdot D_{mtE}^{-1} = J_{O_2/mX} \cdot D_{mtE}^{-1}$ ; (3)  $J_{O_2/mtE} =$   
 1062  $J_{V,O_2} \cdot C_{NX}^{-1} \cdot mtE_{NX}^{-1} = I_{O_2/NX} \cdot mtE_{NX}^{-1}$ ; (4)  $J_{O_2/mtE} = I_{O_2} \cdot mtE^{-1}$ . The mt-elementary unit [mtEU] varies depending  
 1063 on the mt-marker.

**Table 5. Sample types, X, abbreviations, and quantification.**

Identity of sample	$X$	$N_X$	Mass <sup>a</sup>	Volume	mt-Marker
mitochondrial preparation		[x]	[kg]	[m <sup>3</sup> ]	[mtEU]
isolated mitochondria	imt		$m_{mt}$	$V_{mt}$	$mtE$
tissue homogenate	thom		$m_{thom}$		$mtE_{thom}$
permeabilized tissue	pti		$m_{pti}$		$mtE_{pti}$
permeabilized fibre	pfi		$m_{pfi}$		$mtE_{pfi}$
permeabilized cell	pce	$N_{pce}$	$M_{pce}$	$V_{pce}$	$mtE_{pce}$
cells <sup>b</sup>	ce	$N_{ce}$	$M_{ce}$	$V_{ce}$	$mtE_{ce}$
intact cell, viable cell	vce	$N_{vce}$	$M_{vce}$	$V_{vce}$	
dead cell	dce	$N_{dce}$	$M_{dce}$	$V_{dce}$	
organism	org	$N_{org}$	$M_{org}$	$V_{org}$	

<sup>a</sup> Instead of mass, the wet weight or dry weight is frequently stated,  $W_w$  or  $W_d$ .  $m_X$  is mass of the sample [kg],  $M_X$  is mass of the object [kg·x<sup>-1</sup>] (Table 4).

<sup>b</sup> Total cell count,  $N_{ce} = N_{vce} + N_{dce}$

#### 4.1. Flow: per object

**4.1.1. Number concentration,  $C_{NX}$ :** Normalization per sample concentration is routinely required to report respiratory data.  $C_{NX}$  is the experimental number concentration of sample  $X$ . In the case of animals, *e.g.*, nematodes,  $C_{NX} = N_X/V$  [x·L<sup>-1</sup>], where  $N_X$  is the number of organisms in the chamber. Similarly, the number of cells per chamber volume is the number concentration of permeabilized or intact cells  $C_{Nce} = N_{ce}/V$  [x·L<sup>-1</sup>], where  $N_{ce}$  is the number of cells in the chamber (Table 4).

**4.1.2. Flow per object,  $I_{O_2/NX}$ :**  $O_2$  flow per cell is calculated from volume-specific  $O_2$  flux,  $J_{V,O_2}$  [nmol·s<sup>-1</sup>·L<sup>-1</sup>] (per  $V$  of the measurement chamber [L]), divided by the number concentration of cells. The total cell count is the sum of viable and dead cells,  $N_{ce} = N_{vce} + N_{dce}$  (Table 5). The cell viability index,  $VI = N_{vce}/N_{ce}$ , is the ratio of viable cells ( $N_{vce}$ ; before experimental permeabilization) per total cell count. After experimental permeabilization, all cells are permeabilized,  $N_{pce} = N_{ce}$ . The cell viability index can be used to normalize respiration for the number of cells that have been viable before experimental permeabilization,  $I_{O_2/Nvce} = I_{O_2/Nce}/VI$ , considering that mitochondrial respiratory dysfunction in dead cells should be eliminated as a confounding factor.

The complexity changes when the object is a whole organism studied as an experimental model. The scaling law in respiratory physiology reveals a strong interaction between  $O_2$  flow and individual body mass: *basal* metabolic rate (flow) does not increase linearly with body mass, whereas *maximum* mass-specific  $O_2$  flux,  $\dot{V}_{O_2max}$  or  $\dot{V}_{O_2peak}$ , is approximately constant across a large range of individual body mass (Weibel and Hoppeler 2005). Individuals, breeds and species, however, deviate substantially from this relationship.  $\dot{V}_{O_2peak}$  of human endurance athletes is 60 to 80 mL  $O_2$ ·min<sup>-1</sup>·kg<sup>-1</sup> body mass, converted to  $J_{O_2peak/Morg}$  of 45 to 60 nmol·s<sup>-1</sup>·g<sup>-1</sup> (Gnaiger 2014; Table 6).



#### 4.2. Size-specific flux: per sample size

**4.2.1. Sample concentration,  $C_{mX}$ :** Considering permeabilized tissue, homogenate or cells as the sample,  $X$ , the sample mass is  $m_X$  [mg], which is frequently measured as wet or dry weight,  $W_w$  or  $W_d$  [mg], respectively, or as amount of protein,  $m_{\text{Protein}}$ . The sample concentration is the mass of the subsample per volume of the measurement chamber,  $C_{mX} = m_X/V$  [ $\text{g}\cdot\text{L}^{-1} = \text{mg}\cdot\text{mL}^{-1}$ ].  $X$  is the type of sample—isolated mitochondria, tissue homogenate, permeabilized fibres or cells (**Table 5**).

**4.2.2. Size-specific flux:** Cellular  $\text{O}_2$  flow can be compared between cells of identical size. To take into account changes and differences in cell size, normalization is required to obtain cell size-specific or mitochondrial marker-specific  $\text{O}_2$  flux (Renner *et al.* 2003).

- **Mass-specific flux,  $J_{\text{O}_2/mX}$  [ $\text{mol}\cdot\text{s}^{-1}\cdot\text{kg}^{-1}$ ]:** Mass-specific flux is obtained by expressing respiration per mass of sample,  $m_X$  [mg]. Flow per cell is divided by mass per cell,  $J_{\text{O}_2/mce} = I_{\text{O}_2/Nce}/M_{Nce}$ . Or chamber volume-specific flux,  $J_{V,\text{O}_2}$ , is divided by mass concentration of  $X$  in the chamber,  $J_{\text{O}_2/mX} = J_{V,\text{O}_2}/C_{mX}$ .
- **Cell volume-specific flux,  $J_{\text{O}_2/VX}$  [ $\text{mol}\cdot\text{s}^{-1}\cdot\text{m}^{-3}$ ]:** Sample volume-specific flux is obtained by expressing respiration per volume of sample. For example, in the case of using cells as sample will be the volume of cells added to the chamber (**Figure 6**).

If size-specific  $\text{O}_2$  flux is constant and independent of sample size, then there is no interaction between the subsystems. For example, a 1.5 mg and a 3.0 mg muscle sample respire at identical mass-specific flux. Mass-specific  $\text{O}_2$  flux, however, may change with the mass of a tissue sample, cells or isolated mitochondria in the measuring chamber, in which the nature of the interaction becomes an issue. Therefore, cell density must be optimized, particularly in experiments carried out in wells, considering the confluency of the cell monolayer or clumps of cells (Salabei *et al.* 2014).

#### 4.3. Marker-specific flux: per mitochondrial content

Tissues can contain multiple cell populations that may have distinct mitochondrial subtypes. Mitochondria undergo dynamic fission and fusion cycles, and can exist in multiple stages and sizes that may be altered by a range of factors. The isolation of mitochondria (often achieved through differential centrifugation) can therefore yield a subsample of the mitochondrial types present in a tissue, depending on the isolation protocols utilized (*e.g.*, centrifugation speed). This possible bias should be taken into account when planning experiments using isolated mitochondria. Different sizes of mitochondria are enriched at specific centrifugation speeds, which can be used strategically for isolation of mitochondrial subpopulations.

Part of the mitochondrial content of a tissue is lost during preparation of isolated mitochondria. The fraction of isolated mitochondria obtained from a tissue sample is expressed as mitochondrial recovery. At a high mitochondrial recovery the fraction of isolated mitochondria is more representative of the total mitochondrial population than in preparations characterized by low recovery. Determination of the mitochondrial recovery and yield is based on measurement of the concentration of a mitochondrial marker in the stock of isolated mitochondria,  $C_{mtE,stock}$ , and crude tissue homogenate,  $C_{mtE,thom}$ , which simultaneously provides information on the specific mitochondrial density in the sample,  $D_{mtE}$  (**Table 4**).

When discussing concepts on normalization, it is essential to consider the question of the study. If the study aims at comparing tissue performance—such as the effects of a treatment on a specific tissue, then normalization for tissue mass or protein content is appropriate. However, if the aim is to find differences on mitochondrial function independent of mitochondrial density (**Table 4**), then normalization to a mitochondrial marker is imperative (**Figure 6**). One cannot assume that quantitative changes in various markers—such as mitochondrial proteins—necessarily occur in parallel with one another. It should be established that the marker chosen is not selectively altered by the performed treatment. In conclusion, the normalization must reflect the question under investigation to reach a satisfying answer. On the other hand, the goal of comparing results across projects and institutions requires standardization on normalization for entry into a databank.

**4.3.1. Mitochondrial concentration,  $C_{mtE}$ , and mitochondrial markers:** Mitochondrial organelles comprise a dynamic cellular reticulum in various states of fusion and fission. Hence, the definition of an "amount" of mitochondria is often misconceived: mitochondria cannot be counted reliably as a number of occurring elementary components. Therefore, quantification of the "amount" of

1150 mitochondria depends on the measurement of chosen mitochondrial markers. ‘Mitochondria are the  
 1151 structural and functional elementary units of cell respiration’ (Gnaiger 2014). The quantity of a  
 1152 mitochondrial marker can reflect the amount of *mitochondrial elementary components*,  $mtE$ , expressed  
 1153 in various mitochondrial elementary units [mtEU] specific for each measured mt-marker (**Table 4**).  
 1154 However, since mitochondrial quality may change in response to stimuli—particularly in mitochondrial  
 1155 dysfunction (Campos *et al.* 2017) and after exercise training (Pesta *et al.* 2011) and during aging (Daum  
 1156 *et al.* 2013)—some markers can vary while others are unchanged: (1) Mitochondrial volume and  
 1157 membrane area are structural markers, whereas mitochondrial protein mass is commonly used as a  
 1158 marker for isolated mitochondria. (2) Molecular and enzymatic mitochondrial markers (amounts or  
 1159 activities) can be selected as matrix markers, *e.g.*, citrate synthase activity, mtDNA; mtIM-markers, *e.g.*,  
 1160 cytochrome *c* oxidase activity,  $aa_3$  content, cardiolipin, or mtOM-markers, *e.g.*, the voltage-dependent  
 1161 anion channel (VDAC), TOM20. (3) Extending the measurement of mitochondrial marker enzyme  
 1162 activity to mitochondrial pathway capacity, ET- or OXPHOS-capacity can be considered as an  
 1163 integrative functional mitochondrial marker.

1164 Depending on the type of mitochondrial marker, the mitochondrial elementary component,  $mtE$ ,  
 1165 is expressed in marker-specific units. Mitochondrial concentration in the measurement chamber and the  
 1166 tissue of origin are quantified as (1) a quantity for normalization in functional analyses,  $C_{mtE}$ , and (2) a  
 1167 physiological output that is the result of mitochondrial biogenesis and degradation,  $D_{mtE}$ , respectively  
 1168 (**Table 4**). It is recommended, therefore, to distinguish *experimental mitochondrial concentration*,  $C_{mtE}$   
 1169  $= mtE/V$  and *physiological mitochondrial density*,  $D_{mtE} = mtE/m_X$ . Then mitochondrial density is the  
 1170 amount of mitochondrial elementary components per mass of tissue, which is a biological variable  
 1171 (**Figure 6**). The experimental variable is mitochondrial density multiplied by sample mass concentration  
 1172 in the measuring chamber,  $C_{mtE} = D_{mtE} \cdot C_{m_X}$ , or mitochondrial content multiplied by sample number  
 1173 concentration,  $C_{mtE} = mtE_X \cdot C_{N_X}$  (**Table 4**).

1174 **4.3.2. mt-Marker-specific flux,  $J_{O_2/mtE}$ :** Volume-specific metabolic  $O_2$  flux depends on: (1) the  
 1175 sample concentration in the volume of the instrument chamber,  $C_{m_X}$ , or  $C_{N_X}$ ; (2) the mitochondrial  
 1176 density in the sample,  $D_{mtE} = mtE/m_X$  or  $mtE_X = mtE/N_X$ ; and (3) the specific mitochondrial activity or  
 1177 performance per elementary mitochondrial unit,  $J_{O_2/mtE} = J_{V,O_2}/C_{mtE}$  [ $mol \cdot s^{-1} \cdot mtEU^{-1}$ ] (**Table 4**).  
 1178 Obviously, the numerical results for  $J_{O_2/mtE}$  vary with the type of mitochondrial marker chosen for  
 1179 measurement of  $mtE$  and  $C_{mtE} = mtE/V$  [ $mtEU \cdot m^{-3}$ ].

1180 Different methods are implicated in the quantification of mitochondrial markers and have  
 1181 different strengths. Some problems are common for all mitochondrial markers,  $mtE$ : (1) Accuracy of  
 1182 measurement is crucial, since even a highly accurate and reproducible measurement of  $O_2$  flux results  
 1183 in an inaccurate and noisy expression if normalized by a biased and noisy measurement of a  
 1184 mitochondrial marker. This problem is acute in mitochondrial respiration because the denominators used  
 1185 (the mitochondrial markers) are often small moieties of which accurate and precise determination is  
 1186 difficult. This problem can be avoided when  $O_2$  fluxes measured in substrate-uncoupler-inhibitor  
 1187 titration protocols are normalized for flux in a defined respiratory reference state, which is used as an  
 1188 *internal* marker and yields flux control ratios, *FCRs*. *FCRs* are independent of externally measured  
 1189 markers and, therefore, are statistically robust, considering the limitations of ratios in general (Jasienski  
 1190 and Bazzaz 1999). *FCRs* indicate qualitative changes of mitochondrial respiratory control, with highest  
 1191 quantitative resolution, separating the effect of mitochondrial density or concentration on  $J_{O_2/m_X}$  and  
 1192  $J_{O_2/N_X}$  from that of function per elementary mitochondrial marker,  $J_{O_2/mtE}$  (Pesta *et al.* 2011; Gnaiger  
 1193 2014). (2) If mitochondrial quality does not change and only the amount of mitochondria varies as a  
 1194 determinant of mass-specific flux, any marker is equally qualified in principle; then in practice selection  
 1195 of the optimum marker depends only on the accuracy and precision of measurement of the mitochondrial  
 1196 marker. (3) If mitochondrial flux control ratios change, then there may not be any best mitochondrial  
 1197 marker. In general, measurement of multiple mitochondrial markers enables a comparison and  
 1198 evaluation of normalization for a variety of mitochondrial markers. Particularly during postnatal  
 1199 development, the activity of marker enzymes—such as cytochrome *c* oxidase and citrate synthase—  
 1200 follows different time courses (Drahota *et al.* 2004). Evaluation of mitochondrial markers in healthy  
 1201 controls is insufficient for providing guidelines for application in the diagnosis of pathological states  
 1202 and specific treatments.

1203 In line with the concept of the respiratory control ratio (Chance and Williams 1955a), the most  
 1204 readily used normalization is that of flux control ratios and flux control factors (Gnaiger 2014). Selection  
 1205 of the state of maximum flux in a protocol as the reference state has the advantages of: (1) internal

1206 normalization; (2) statistically validated linearization of the response in the range of 0 to 1; and (3)  
 1207 consideration of maximum flux for integrating a large number of elementary steps in the OXPHOS- or  
 1208 ET-pathways. This reduces the risk of selecting a functional marker that is specifically altered by the  
 1209 treatment or pathology, yet increases the chance that the highly integrative pathway is disproportionately  
 1210 affected, *e.g.*, the OXPHOS- rather than ET-pathway in case of an enzymatic defect in the  
 1211 phosphorylation-pathway. In this case, additional information can be obtained by reporting flux control  
 1212 ratios based on a reference state which indicates stable tissue-mass specific flux.

1213 Stereological determination of mitochondrial content via two-dimensional transmission electron  
 1214 microscopy can have limitations due to the dynamics of mitochondrial size (Meinild Lundby *et al.*  
 1215 2017). Accurate determination of three-dimensional volume by two-dimensional microscopy can be  
 1216 both time consuming and statistically challenging (Larsen *et al.* 2012).

1217 The validity of using mitochondrial marker enzymes (citrate synthase activity, CI to CIV amount  
 1218 or activity) for normalization of flux is limited in part by the same factors that apply to flux control  
 1219 ratios. Strong correlations between various mitochondrial markers and citrate synthase activity  
 1220 (Reichmann *et al.* 1985; Boushel *et al.* 2007; Mogensen *et al.* 2007) are expected in a specific tissue of  
 1221 healthy persons and in disease states not specifically targeting citrate synthase. Citrate synthase activity  
 1222 is acutely modifiable by exercise (Tonkonogi *et al.* 1997; Leek *et al.* 2001). Evaluation of mitochondrial  
 1223 markers related to a selected age and sex cohort cannot be extrapolated to provide recommendations for  
 1224 normalization in respirometric diagnosis of disease, in different states of development and ageing,  
 1225 different cell types, tissues, and species. mtDNA normalized to nDNA via qPCR is correlated to  
 1226 functional mitochondrial markers including OXPHOS- and ET-capacity in some cases (Puntschart *et al.*  
 1227 1995; Wang *et al.* 1999; Menshikova *et al.* 2006; Boushel *et al.* 2007; Ehinger *et al.* 2015), but lack of  
 1228 such correlations have been reported (Menshikova *et al.* 2005; Schultz and Wiesner 2000; Pesta *et al.*  
 1229 2011). Several studies indicate a strong correlation between cardiolipin content and increase in  
 1230 mitochondrial function with exercise (Menshikova *et al.* 2005; Menshikova *et al.* 2007; Larsen *et al.*  
 1231 2012; Faber *et al.* 2014), but it has not been evaluated as a general mitochondrial biomarker in disease.  
 1232 With no single best mitochondrial marker, a good strategy is to quantify several different biomarkers to  
 1233 minimize the decorrelating effects caused by diseases, treatments, or other factors. Determination of  
 1234 multiple markers, particularly a matrix marker and a marker from the mtIM, allows tracking changes in  
 1235 mitochondrial quality defined by their ratio.

## 1236 5. Normalization of rate per system

### 1237 5.1. Flow: per chamber

1238 The experimental system (experimental chamber) is part of the measurement instrument,  
 1239 separated from the environment as an isolated, closed, open, isothermal or non-isothermal system  
 1240 (Table 4). Reporting O<sub>2</sub> flows per respiratory chamber,  $I_{O_2}$  [nmol·s<sup>-1</sup>], restricts the analysis to intra-  
 1241 experimental comparison of relative differences.

### 1242 5.2. Flux: per chamber volume

1243 **5.2.1. System-specific flux,  $J_{V,O_2}$ :** We distinguish between (1) the *system* with volume  $V$  and mass  
 1244  $m$  defined by the system boundaries, and (2) the *sample* or *objects* with volume  $V_X$  and mass  $m_X$  that are  
 1245 enclosed in the experimental chamber (Figure 6). Metabolic O<sub>2</sub> flow per object,  $I_{O_2/N_X}$ , is the total O<sub>2</sub>  
 1246 flow in the system divided by the number of objects,  $N_X$ , in the system.  $I_{O_2/N_X}$  increases as the mass of  
 1247 the object is increased. Sample mass-specific O<sub>2</sub> flux,  $J_{O_2/m_X}$  should be independent of the mass of the  
 1248 sample studied in the instrument chamber, but system volume-specific O<sub>2</sub> flux,  $J_{V,O_2}$  (per volume of the  
 1249 instrument chamber), increases in proportion to the mass of the sample in the chamber. Whereas  $J_{V,O_2}$   
 1250 depends on mass-concentration of the sample in the chamber, it should be independent of the chamber  
 1251 (system) volume at constant sample mass. There are practical limitations to increase the mass-  
 1252 concentration of the sample in the chamber, when one is concerned about crowding effects and  
 1253 instrumental time resolution.

1254 **5.2.2. Advancement per volume:** When the reactor volume does not change during the reaction,  
 1255 which is typical for liquid phase reactions, the volume-specific flux of a chemical reaction  $r$  is the time

1262 derivative of the advancement of the reaction per unit volume,  $J_{V,rB} = d_r \xi_B / dt \cdot V^{-1}$  [(mol·s<sup>-1</sup>)·L<sup>-1</sup>]. The *rate*  
 1263 *of concentration change* is  $dc_B/dt$  [(mol·L<sup>-1</sup>)·s<sup>-1</sup>], where concentration is  $c_B = n_B/V$ . There is a difference  
 1264 between (1)  $J_{V,rO_2}$  [mol·s<sup>-1</sup>·L<sup>-1</sup>] and (2) rate of concentration change [mol·L<sup>-1</sup>·s<sup>-1</sup>]. These merge to a single  
 1265 expression only in closed systems. In open systems, internal transformations (catabolic flux, O<sub>2</sub>  
 1266 consumption) are distinguished from external flux (such as O<sub>2</sub> supply). External fluxes of all substances  
 1267 are zero in closed systems. In a closed chamber O<sub>2</sub> consumption (internal flux of catabolic reactions  $k$ ),  
 1268  $I_{kO_2}$  [pmol·s<sup>-1</sup>], causes a decline of the amount of O<sub>2</sub> in the system,  $n_{O_2}$  [nmol]. Normalization of these  
 1269 quantities for the volume of the system,  $V$  [L  $\equiv$  dm<sup>3</sup>], yields volume-specific O<sub>2</sub> flux,  $J_{V,kO_2} = I_{kO_2}/V$   
 1270 [nmol·s<sup>-1</sup>·L<sup>-1</sup>], and O<sub>2</sub> concentration, [O<sub>2</sub>] or  $c_{O_2} = n_{O_2}/V$  [ $\mu$ mol·L<sup>-1</sup> =  $\mu$ M = nmol·mL<sup>-1</sup>]. Instrumental  
 1271 background O<sub>2</sub> flux is due to external flux into a non-ideal closed respirometer; then total volume-  
 1272 specific flux has to be corrected for instrumental background O<sub>2</sub> flux—O<sub>2</sub> diffusion into or out of the  
 1273 instrumental chamber.  $J_{V,kO_2}$  is relevant mainly for methodological reasons and should be compared with  
 1274 the accuracy of instrumental resolution of background-corrected flux, *e.g.*,  $\pm 1$  nmol·s<sup>-1</sup>·L<sup>-1</sup> (Gnaiger  
 1275 2001). ‘Metabolic’ or catabolic indicates O<sub>2</sub> flux,  $J_{kO_2}$ , corrected for: (1) instrumental background O<sub>2</sub>  
 1276 flux; (2) chemical background O<sub>2</sub> flux due to autoxidation of chemical components added to the  
 1277 incubation medium; and (3) *Rox* for O<sub>2</sub>-consuming side reactions unrelated to the catabolic pathway  $k$ .

1278  
1279

## 1280 6. Conversion of units

1281  
1282  
1283  
1284  
1285  
1286  
1287  
1288

Many different units have been used to report the O<sub>2</sub> consumption rate, OCR (Table 6). SI base  
 units provide the common reference to introduce the theoretical principles (Figure 6), and are used with  
 appropriately chosen *SI* prefixes to express numerical data in the most practical format, with an effort  
 towards unification within specific areas of application (Table 7). Reporting data in *SI* units—including  
 the mole [mol], coulomb [C], joule [J], and second [s]—should be encouraged, particularly by journals  
 which propose the use of *SI* units.

1289  
1290  
1291  
1292

**Table 6. Conversion of various formats and units used in respirometry and ergometry.**  $e^-$  is the number of electrons or reducing equivalents.  $z_B$  is the charge number of entity B.

Format	1 Unit		Multiplication factor	<i>SI</i> -unit	Notes
$\underline{n}$	ng.atom O·s <sup>-1</sup>	(2 $e^-$ )	0.5	nmol O <sub>2</sub> ·s <sup>-1</sup>	
$\underline{n}$	ng.atom O·min <sup>-1</sup>	(2 $e^-$ )	8.33	pmol O <sub>2</sub> ·s <sup>-1</sup>	
$\underline{n}$	natom O·min <sup>-1</sup>	(2 $e^-$ )	8.33	pmol O <sub>2</sub> ·s <sup>-1</sup>	
$\underline{n}$	nmol O <sub>2</sub> ·min <sup>-1</sup>	(4 $e^-$ )	16.67	pmol O <sub>2</sub> ·s <sup>-1</sup>	
$\underline{n}$	nmol O <sub>2</sub> ·h <sup>-1</sup>	(4 $e^-$ )	0.2778	pmol O <sub>2</sub> ·s <sup>-1</sup>	
$\underline{V}$ to $\underline{n}$	mL O <sub>2</sub> ·min <sup>-1</sup> at STPD <sup>a</sup>		0.744	$\mu$ mol O <sub>2</sub> ·s <sup>-1</sup>	1
$\underline{e}$ to $\underline{n}$	W = J/s at -470 kJ/mol O <sub>2</sub>		-2.128	$\mu$ mol O <sub>2</sub> ·s <sup>-1</sup>	
$\underline{e}$ to $\underline{n}$	mA = mC·s <sup>-1</sup>	( $z_{H^+} = 1$ )	10.36	nmol H <sup>+</sup> ·s <sup>-1</sup>	2
$\underline{e}$ to $\underline{n}$	mA = mC·s <sup>-1</sup>	( $z_{O_2} = 4$ )	2.59	nmol O <sub>2</sub> ·s <sup>-1</sup>	2
$\underline{n}$ to $\underline{e}$	nmol H <sup>+</sup> ·s <sup>-1</sup>	( $z_{H^+} = 1$ )	0.09649	mA	3
$\underline{n}$ to $\underline{e}$	nmol O <sub>2</sub> ·s <sup>-1</sup>	( $z_{O_2} = 4$ )	0.38594	mA	3

- 1293 1 At standard temperature and pressure dry (STPD: 0 °C = 273.15 K and 1 atm = 101.325 kPa =  
 1294 760 mmHg), the molar volume of an ideal gas,  $V_m$ , and  $V_{m,O_2}$  is 22.414 and 22.392 L·mol<sup>-1</sup>,  
 1295 respectively. Rounded to three decimal places, both values yield the conversion factor of 0.744.  
 1296 For comparison at normal temperature and pressure dry (NTPD: 20 °C),  $V_{m,O_2}$  is 24.038 L·mol<sup>-1</sup>.  
 1297 Note that the *SI* standard pressure is 100 kPa.  
 1298 2 The multiplication factor is  $10^6/(z_B \cdot F)$ .  
 1299 3 The multiplication factor is  $z_B \cdot F/10^6$ .  
 1300

1301 **Table 7. Conversion of units with preservation of numerical values.**

Name	Frequently used unit	Equivalent unit	Notes
volume-specific flux, $J_{V,O_2}$	$\text{pmol}\cdot\text{s}^{-1}\cdot\text{mL}^{-1}$ $\text{mmol}\cdot\text{s}^{-1}\cdot\text{L}^{-1}$	$\text{nmol}\cdot\text{s}^{-1}\cdot\text{L}^{-1}$ $\text{mol}\cdot\text{s}^{-1}\cdot\text{m}^{-3}$	1
cell-specific flow, $I_{O_2/\text{cell}}$	$\text{pmol}\cdot\text{s}^{-1}\cdot 10^{-6}$ cells	$\text{amol}\cdot\text{s}^{-1}\cdot\text{cell}^{-1}$	2
	$\text{pmol}\cdot\text{s}^{-1}\cdot 10^{-9}$ cells	$\text{zmol}\cdot\text{s}^{-1}\cdot\text{cell}^{-1}$	3
cell number concentration, $C_{Nce}$	$10^6$ cells $\cdot\text{mL}^{-1}$	$10^9$ cells $\cdot\text{L}^{-1}$	
mitochondrial protein concentration, $C_{mtE}$	$0.1$ mg $\cdot\text{mL}^{-1}$	$0.1$ g $\cdot\text{L}^{-1}$	
mass-specific flux, $J_{O_2/m}$	$\text{pmol}\cdot\text{s}^{-1}\cdot\text{mg}^{-1}$	$\text{nmol}\cdot\text{s}^{-1}\cdot\text{g}^{-1}$	4
catabolic power, $P_k$	$\mu\text{W}\cdot 10^{-6}$ cells	$\text{pW}\cdot\text{cell}^{-1}$	1
volume	1,000 L	$\text{m}^3$ (1,000 kg)	
	L	$\text{dm}^3$ (kg)	
	mL	$\text{cm}^3$ (g)	
	$\mu\text{L}$	$\text{mm}^3$ (mg)	
	fL	$\mu\text{m}^3$ (pg)	5
amount of substance concentration	$\text{M} = \text{mol}\cdot\text{L}^{-1}$	$\text{mol}\cdot\text{dm}^{-3}$	

1302 1 pmol: picomole =  $10^{-12}$  mol1303 2 amol: attomole =  $10^{-18}$  mol1304 3 zmol: zeptomole =  $10^{-21}$  mol

1305

1306 Although volume is expressed as  $\text{m}^3$  using the *SI* base unit, the litre [ $\text{dm}^3$ ] is a conventional unit  
 1307 of volume for concentration and is used for most solution chemical kinetics. If one multiplies  $I_{O_2/Nce}$  by  
 1308  $C_{Nce}$ , then the result will not only be the amount of  $\text{O}_2$  [mol] consumed per time [ $\text{s}^{-1}$ ] in one litre [ $\text{L}^{-1}$ ],  
 1309 but also the change in  $\text{O}_2$  concentration per second (for any volume of an ideally closed system). This  
 1310 is ideal for kinetic modeling as it blends with chemical rate equations where concentrations are typically  
 1311 expressed in  $\text{mol}\cdot\text{L}^{-1}$  (Wagner *et al.* 2011). In studies of multinuclear cells—such as differentiated  
 1312 skeletal muscle cells—it is easy to determine the number of nuclei but not the total number of cells. A  
 1313 generalized concept, therefore, is obtained by substituting cells by nuclei as the sample entity. This does  
 1314 not hold, however, for enucleated platelets.

1315 For studies of cells, we recommend that respiration be expressed, as far as possible, as: (1)  $\text{O}_2$   
 1316 flux normalized for a mitochondrial marker, for separation of the effects of mitochondrial quality and  
 1317 content on cell respiration (this includes *FCRs* as a normalization for a functional mitochondrial  
 1318 marker); (2)  $\text{O}_2$  flux in units of cell volume or mass, for comparison of respiration of cells with different  
 1319 cell size (Renner *et al.* 2003) and with studies on tissue preparations, and (3)  $\text{O}_2$  flow in units of attomole  
 1320 ( $10^{-18}$  mol) of  $\text{O}_2$  consumed in a second by each cell [ $\text{amol}\cdot\text{s}^{-1}\cdot\text{cell}^{-1}$ ], numerically equivalent to  
 1321 [ $\text{pmol}\cdot\text{s}^{-1}\cdot 10^{-6}$  cells]. This convention allows information to be easily used when designing experiments  
 1322 in which  $\text{O}_2$  flow must be considered. For example, to estimate the volume-specific  $\text{O}_2$  flux in an  
 1323 instrument chamber that would be expected at a particular cell number concentration, one simply needs  
 1324 to multiply the flow per cell by the number of cells per volume of interest. This provides the amount of  
 1325  $\text{O}_2$  [mol] consumed per time [ $\text{s}^{-1}$ ] per unit volume [ $\text{L}^{-1}$ ]. At an  $\text{O}_2$  flow of  $100$   $\text{amol}\cdot\text{s}^{-1}\cdot\text{cell}^{-1}$  and a cell  
 1326 density of  $10^9$  cells $\cdot\text{L}^{-1}$  ( $10^6$  cells $\cdot\text{mL}^{-1}$ ), the volume-specific  $\text{O}_2$  flux is  $100$   $\text{nmol}\cdot\text{s}^{-1}\cdot\text{L}^{-1}$  ( $100$   
 1327  $\text{pmol}\cdot\text{s}^{-1}\cdot\text{mL}^{-1}$ ).

1328 ET-capacity in human cell types including HEK 293, primary HUVEC and fibroblasts ranges  
 1329 from  $50$  to  $180$   $\text{amol}\cdot\text{s}^{-1}\cdot\text{cell}^{-1}$ , measured in intact cells in the noncoupled state (see Gnaiger 2014). At  
 1330  $100$   $\text{amol}\cdot\text{s}^{-1}\cdot\text{cell}^{-1}$  corrected for *Rox*, the current across the mt-membranes,  $I_{H^+e}$ , approximates  $193$   
 1331  $\text{pA}\cdot\text{cell}^{-1}$  or  $0.2$  nA per cell. See Rich (2003) for an extension of quantitative bioenergetics from the  
 1332 molecular to the human scale, with a transmembrane proton flux equivalent to  $520$  A in an adult at a  
 1333 catabolic power of  $-110$  W. Modelling approaches illustrate the link between protonmotive force and  
 1334 currents (Willis *et al.* 2016).

1335 We consider isolated mitochondria as powerhouses and proton pumps as molecular machines to  
 1336 relate experimental results to energy metabolism of the intact cell. The cellular  $\text{P}\gg/\text{O}_2$  based on oxidation

of glycogen is increased by the glycolytic (fermentative) substrate-level phosphorylation of 3 P<sub>»</sub>/Glyc or 0.5 mol P<sub>»</sub> for each mol O<sub>2</sub> consumed in the complete oxidation of a mol glycosyl unit (Glyc). Adding 0.5 to the mitochondrial P<sub>»</sub>/O<sub>2</sub> ratio of 5.4 yields a bioenergetic cell physiological P<sub>»</sub>/O<sub>2</sub> ratio close to 6. Two NADH equivalents are formed during glycolysis and transported from the cytosol into the mitochondrial matrix, either by the malate-aspartate shuttle or by the glycerophosphate shuttle (**Figure 2A**) resulting in different theoretical yields of ATP generated by mitochondria, the energetic cost of which potentially must be taken into account. Considering also substrate-level phosphorylation in the TCA cycle, this high P<sub>»</sub>/O<sub>2</sub> ratio not only reflects proton translocation and OXPHOS studied in isolation, but integrates mitochondrial physiology with energy transformation in the living cell (Gnaiger 1993a).

## 7. Conclusions

Catabolic cell respiration is the process of exergonic and exothermic energy transformation in which scalar redox reactions are coupled to vectorial ion translocation across a semipermeable membrane, which separates the small volume of a bacterial cell or mitochondrion from the larger volume of its surroundings. The electrochemical exergy can be partially conserved in the phosphorylation of ADP to ATP or in ion pumping, or dissipated in an electrochemical short-circuit. Respiration is thus clearly distinguished from fermentation as the counterpart of cellular core energy metabolism. An O<sub>2</sub> flux balance scheme illustrates the relationships and general definitions (**Figures 1 and 2**).

---

### Box 3: Recommendations for studies with mitochondrial preparations

- Normalization of respiratory rates should be provided as far as possible:
  1. *Biophysical normalization*: on a per cell basis as O<sub>2</sub> flow; this may not be possible when dealing with coenocytic organisms or tissues without cross-walls separating individual cells (e.g., filamentous fungi, muscle fibers)
  2. *Cellular normalization*: per g protein; per cell- or tissue-mass as mass-specific O<sub>2</sub> flux; per cell volume as cell volume-specific flux
  3. *Mitochondrial normalization*: per mitochondrial marker as mt-specific flux.
- With information on cell size and the use of multiple normalizations, maximum potential information is available (Renner *et al.* 2003; Wagner *et al.* 2011; Gnaiger 2014). Reporting flow in a respiratory chamber [nmol·s<sup>-1</sup>] is discouraged, since it restricts the analysis to intra-experimental comparison of relative (qualitative) differences.
- Catabolic mitochondrial respiration is distinguished from residual O<sub>2</sub> consumption. Fluxes in mitochondrial coupling states should be, as far as possible, corrected for residual O<sub>2</sub> consumption.
- Different mechanisms of uncoupling should be distinguished by defined terms. The tightness of coupling relates to these uncoupling mechanisms, whereas the coupling stoichiometry varies as a function the substrate type involved in ET-pathways with either three or two redox proton pumps operating in series. Separation of tightness of coupling from the pathway-dependent coupling stoichiometry is possible only when the substrate type undergoing oxidation remains the same for respiration in LEAK-, OXPHOS-, and ET-states. In studies of the tightness of coupling, therefore, simple substrate-inhibitor combinations should be applied to exclude a shift in substrate competition which may occur when providing physiological substrate cocktails.
- In studies of isolated mitochondria, the mitochondrial recovery and yield should be reported. Experimental criteria for evaluation of purity versus integrity should be considered. Mitochondrial markers—such as citrate synthase activity as an enzymatic matrix marker—provide a link to the tissue of origin on the basis of calculating the mitochondrial recovery, *i.e.*, the fraction of mitochondrial marker obtained from a unit mass of tissue. Total mitochondrial protein is frequently applied as a mitochondrial marker, which is restricted to isolated mitochondria.
- In studies of permeabilized cells, the viability of the cell culture or cell suspension of origin should be reported. Normalization should be evaluated for total cell count or viable cell count.
- Terms and symbols are summarized in **Table 8**. Their use will facilitate transdisciplinary communication and support further developments towards a consistent theory of bioenergetics and mitochondrial physiology. Technical terms related to and defined with normal words can be used as index terms in databases, support the creation of ontologies towards semantic information processing

1393 (MitoPedia), and help in communicating analytical findings as impactful data-driven stories.  
 1394 'Making data available without making it understandable may be worse than not making it available  
 1395 at all' (National Academies of Sciences, Engineering, and Medicine 2018). Success will depend on  
 1396 taking next steps: (1) exhaustive text-mining considering Omics data and functional data; (2) network  
 1397 analysis of Omics data with bioinformatics tools; (3) cross-validation with distinct bioinformatics  
 1398 approaches; (4) correlation with functional data; (5) guidelines for biological validation of network  
 1399 data. This is a call to carefully contribute to FAIR principles (Findable, Accessible, Interoperable,  
 1400 Reusable) for the sharing of scientific data.  
 1401

1402  
 1403 **Table 8. Terms, symbols, and units.**  
 1404

1405	1406	1407	1408	1409
Term	Symbol	Unit	Links and comments	
1409	AOX		Figure 2B	
1410	$n_B$	[mol]		
1411	$Y_{P\gg/O_2}$		P $\gg$ /O <sub>2</sub> ratio measured in any respiratory state	
1412				
1413	k		Figure 1 and 3	
1414	$J_{kO_2}$	<i>varies</i>	Figure 1 and 3	
1415	$N_{ce}$	[x]	$N_{ce} = N_{vce} + N_{dce}$ ; Table 5	
1416	$J_{rO_2}$	<i>varies</i>	Figure 1	
1417	VI		$VI = N_{vce}/N_{ce} = 1 - N_{dce}/N_{ce}$	
1418	$z_B$		Table 6; $z_{O_2} = 4$	
1419	CI to CIV		respiratory ET Complexes; Figure 2B	
1420				
1421	$c_B = n_B \cdot V^{-1}$ ; [B]	[mol·m <sup>-3</sup> ]	Box 2	
1422	CCS		Section 2.4.1	
1423	$N_{dce}$	[x]	non-viable cells, loss of plasma membrane barrier function; Table 5	
1424				
1425	$\underline{e}$	[C]	Table 6	
1426	ETS		state; Figure 2B, Figure 4	
1427	$I_B$	[mol·s <sup>-1</sup> ]	system-related extensive quantity; Figure 6	
1428				
1429	$J_B$	<i>varies</i>	size-specific quantity; Figure 6	
1430	P <sub>i</sub>		Figure 2C	
1431	PiC		Figure 2C	
1432				
1433	$N_{vce}$	[x]	viable cells, intact of plasma membrane barrier function; Table 5	
1434				
1435	LEAK		state; Table 1, Figure 4	
1436	$\underline{m}$	[kg]	Table 4, Figure 6	
1437	$m_X$	[kg]	Table 4	
1438	$m_d$	[kg]	mass of sample X; Figure 6 (frequently called dry weight)	
1439				
1440	$m_w$	[kg]	mass of sample X; Figure 6 (frequently called wet weight)	
1441				
1442	$M_X = m_X \cdot N_X^{-1}$	[kg·x <sup>-1</sup> ]	mass of entity X; Table 4	
1443	MITOCARTA		<a href="https://www.broadinstitute.org/scientific-community/science/programs/metabolic-disease-program/publications/mitocarta/mitocarta-in-0">https://www.broadinstitute.org/scientific-community/science/programs/metabolic-disease-program/publications/mitocarta/mitocarta-in-0</a>	
1444				
1445				
1446				
1447				

1448	MitoPedia			<a href="http://www.bioblast.at/index.php/MitoPedia">http://www.bioblast.at/index.php/MitoPedia</a>
1449	mitochondria or mitochondrial	mt		Box 1
1450	mitochondrial DNA	mtDNA		Box 1
1451	mitochondrial concentration	$C_{mtE} = mtE \cdot V^{-1}$	[mtEU·m <sup>-3</sup> ]	Table 4
1452	mitochondrial content	$mtE_X$	[mtEU·x <sup>-1</sup> ]	$mtE_X = mtE \cdot N_X^{-1}$ ; Table 4
1453	mitochondrial			
1454	elementary component	$mtE$	[mtEU]	quantity of mt-marker; Table 4
1455	mitochondrial elementary unit	mtEU	<i>varies</i>	specific units for mt-marker; Table 4
1456	mitochondrial inner membrane	mtIM		MIM is widely used; the first M is replaced by mt; Figure 2; Box 1
1457				
1458	mitochondrial outer membrane	mtOM		MOM is widely used; the first M is replaced by mt; Figure 2; Box 1
1459				
1460	mitochondrial recovery	$Y_{mtE}$		fraction of $mtE$ recovered in sample
1461				from the tissue of origin
1462	mitochondrial yield	$Y_{mtE/m}$		mt-yield per tissues mass; $Y_{mtE/m} =$
1463				$Y_{mtE} \cdot D_{mtE}$
1464	molar format	$\underline{n}$	[mol]	Table 6
1465	negative	neg		Figure 4
1466	number concentration of $X$	$C_{NX}$	[x·m <sup>-3</sup> ]	Table 4
1467	number format	$\underline{N}$	[x]	Table 4, Figure 6
1468	number of entities $X$	$N_X$	[x]	Table 4, Figure 6
1469	number of entity B	$N_B$	[x]	Table 4
1470	oxidative phosphorylation	<b>OXPPOS</b>		state; Table 1, Figure 4
1471	oxygen concentration	$c_{O_2} = n_{O_2} \cdot V^{-1}$	[mol·m <sup>-3</sup> ]	[O <sub>2</sub> ]; Section 3.2
1472	oxygen flux, in reaction r	$J_{rO_2}$	<i>varies</i>	Figure 1
1473	pathway control state	PCS		Section 2.2
1474	permeabilized cell number	$N_{pce}$	[x]	experimental permeabilization of plasma membrane; Table 5
1475				
1476	phosphorylation of ADP to ATP	P $\gg$		Section 2.2
1477	P $\gg$ /O <sub>2</sub> ratio	P $\gg$ /O <sub>2</sub>		mechanistic $Y_{P\gg/O_2}$ , calculated from pump stoichiometries; Figure 2B
1478				
1479	positive	pos		Figure 4
1480	proton in the negative compartment	H <sup>+</sup> <sub>neg</sub>		Figure 4
1481	proton in the positive compartment	H <sup>+</sup> <sub>pos</sub>		Figure 4
1482	rate of electron transfer in ET state	$E$		ET-capacity; Table 1
1483	rate of LEAK respiration	$L$		Table 1
1484	rate of oxidative phosphorylation	$P$		OXPPOS capacity; Table 1
1485	rate of residual oxygen consumption	$RO_x$		Table 1, Figure 1
1486	residual oxygen consumption	ROX		state; Table 1
1487	respiratory supercomplex	SC I <sub>n</sub> III <sub>n</sub> IV <sub>n</sub>		supramolecular assemblies composed of variable copy numbers ( $n$ ) of CI, CIII and CIV; Box 1
1488				
1489				
1490	specific mitochondrial density	$D_{mtE} = mtE \cdot m_X^{-1}$	[mtEU·kg <sup>-1</sup> ]	Table 4
1491	substrate-uncoupler-inhibitor-titration protocol	SUIT		##
1492				
1493	volume	$V$	[m <sup>-3</sup> ]	Table 7
1494	volume format	$\underline{V}$	[m <sup>-3</sup> ]	Table 6
1495				

1496  
 1497 Experimentally, respiration is separated in mitochondrial preparations from the interactions with  
 1498 the fermentative pathways of the intact cell. OXPPOS analysis is based on the study of mitochondrial  
 1499 preparations complementary to bioenergetic investigations of intact cells and organisms—from model  
 1500 organisms to the human species including healthy and diseased persons (patients). Different mechanisms  
 1501 of respiratory uncoupling have to be distinguished (**Figure 3**). Metabolic fluxes measured in defined  
 1502 coupling and pathway control states (**Figures 5 and 6**) provide insights into the meaning of cellular and  
 1503 organismic respiration.



1504 The optimal choice for expressing mitochondrial and cell respiration as O<sub>2</sub> flow per biological  
 1505 sample, and normalization for specific tissue-markers (volume, mass, protein) and mitochondrial  
 1506 markers (volume, protein, content, mtDNA, activity of marker enzymes, respiratory reference state) is  
 1507 guided by the scientific question under study. Interpretation of the data depends critically on appropriate  
 1508 normalization (**Figure 6**).

1509 MitoEAGLE can serve as a gateway to better diagnose mitochondrial respiratory adaptations and  
 1510 defects linked to genetic variation, age-related health risks, sex-specific mitochondrial performance,  
 1511 lifestyle with its effects on degenerative diseases, and thermal and chemical environment. The present  
 1512 recommendations on coupling control states and rates, linked to the concept of the protonmotive force,  
 1513 are focused on studies with mitochondrial preparations (**Box 3**). These will be extended in a series of  
 1514 reports on pathway control of mitochondrial respiration, respiratory states in intact cells, and  
 1515 harmonization of experimental procedures.

### 1517 **Acknowledgements**

1518 We thank M. Beno for management assistance. This publication is based upon work from COST Action  
 1519 CA15203 MitoEAGLE, supported by COST (European Cooperation in Science and Technology), and  
 1520 K-Regio project MitoFit (E.G.).

1522 **Competing financial interests:** E.G. is founder and CEO of Oroboros Instruments, Innsbruck, Austria.

### 1524 **References**

- 1525 Altmann R (1894) Die Elementarorganismen und ihre Beziehungen zu den Zellen. Zweite vermehrte Auflage.  
 1526 Verlag Von Veit & Comp, Leipzig:160 pp.
- 1527 Baggeto LG, Testa-Perussini R (1990) Role of acetoin on the regulation of intermediate metabolism of Ehrlich  
 1528 ascites tumor mitochondria: its contribution to membrane cholesterol enrichment modifying passive proton  
 1529 permeability. Arch Biochem Biophys 283:341-8.
- 1530 Beard DA (2005) A biophysical model of the mitochondrial respiratory system and oxidative phosphorylation.  
 1531 PLoS Comput Biol 1(4):e36.
- 1532 Benda C (1898) Weitere Mitteilungen über die Mitochondria. Verh Dtsch Physiol Ges:376-83.
- 1533 Birkedal R, Laasmaa M, Vendelin M (2014) The location of energetic compartments affects energetic  
 1534 communication in cardiomyocytes. Front Physiol 5:376.
- 1535 Blier PU, Dufresne F, Burton RS (2001) Natural selection and the evolution of mtDNA-encoded peptides:  
 1536 evidence for intergenomic co-adaptation. Trends Genet 17:400-6.
- 1537 Blier PU, Guderley HE (1993) Mitochondrial activity in rainbow trout red muscle: the effect of temperature on  
 1538 the ADP-dependence of ATP synthesis. J Exp Biol 176:145-58.
- 1539 Breton S, Beaupré HD, Stewart DT, Hoeh WR, Blier PU (2007) The unusual system of doubly uniparental  
 1540 inheritance of mtDNA: isn't one enough? Trends Genet 23:465-74.
- 1541 Brown GC (1992) Control of respiration and ATP synthesis in mammalian mitochondria and cells. Biochem J  
 1542 284:1-13.
- 1543 Burger G, Gray MW, Forget L, Lang BF (2013) Strikingly bacteria-like and gene-rich mitochondrial genomes  
 1544 throughout jakobid protists. Genome Biol Evol 5:418-38.
- 1545 Calvo SE, Klauser CR, Mootha VK (2016) MitoCarta2.0: an updated inventory of mammalian mitochondrial  
 1546 proteins. Nucleic Acids Research 44:D1251-7.
- 1547 Calvo SE, Julien O, Clauser KR, Shen H, Kamer KJ, Wells JA, Mootha VK (2017) Comparative analysis of  
 1548 mitochondrial N-termini from mouse, human, and yeast. Mol Cell Proteomics 16:512-23.
- 1549 Campos JC, Queliconi BB, Bozi LHM, Bechara LRG, Dourado PMM, Andres AM, Jannig PR, Gomes KMS,  
 1550 Zambelli VO, Rocha-Resende C, Guatimosim S, Brum PC, Mochly-Rosen D, Gottlieb RA, Kowaltowski AJ,  
 1551 Ferreira JCB (2017) Exercise reestablishes autophagic flux and mitochondrial quality control in heart failure.  
 1552 Autophagy 13:1304-317.
- 1553 Canton M, Luvisetto S, Schmehl I, Azzone GF (1995) The nature of mitochondrial respiration and  
 1554 discrimination between membrane and pump properties. Biochem J 310:477-81.
- 1555 Carrico C, Meyer JG, He W, Gibson BW, Verdin E (2018) The mitochondrial acylome emerges: proteomics,  
 1556 regulation by Sirtuins, and metabolic and disease implications. Cell Metab 27:497-512.
- 1557 Chan DC (2006) Mitochondria: dynamic organelles in disease, aging, and development. Cell 125:1241-52.
- 1558 Chance B, Williams GR (1955a) Respiratory enzymes in oxidative phosphorylation. I. Kinetics of oxygen  
 1559 utilization. J Biol Chem 217:383-93.
- 1560 Chance B, Williams GR (1955b) Respiratory enzymes in oxidative phosphorylation: III. The steady state. J Biol  
 1561 Chem 217:409-27.

- 1563 Chance B, Williams GR (1955c) Respiratory enzymes in oxidative phosphorylation. IV. The respiratory chain. J  
1564 Biol Chem 217:429-38.
- 1565 Chance B, Williams GR (1956) The respiratory chain and oxidative phosphorylation. Adv Enzymol Relat Subj  
1566 Biochem 17:65-134.
- 1567 Chowdhury SK, Djordjevic J, Albensi B, Fernyhough P (2015) Simultaneous evaluation of substrate-dependent  
1568 oxygen consumption rates and mitochondrial membrane potential by TMRM and safranin in cortical  
1569 mitochondria. Biosci Rep 36:e00286.
- 1570 Cobb LJ, Lee C, Xiao J, Yen K, Wong RG, Nakamura HK, Mehta HH, Gao Q, Ashur C, Huffman DM, Wan J,  
1571 Muzumdar R, Barzilai N, Cohen P (2016) Naturally occurring mitochondrial-derived peptides are age-  
1572 dependent regulators of apoptosis, insulin sensitivity, and inflammatory markers. Aging (Albany NY) 8:796-  
1573 809.
- 1574 Cohen ER, Cvitas T, Frey JG, Holmström B, Kuchitsu K, Marquardt R, Mills I, Pavese F, Quack M, Stohner J,  
1575 Strauss HL, Takami M, Thor HL (2008) Quantities, units and symbols in physical chemistry, IUPAC Green  
1576 Book, 3rd Edition, 2nd Printing, IUPAC & RSC Publishing, Cambridge.
- 1577 Cooper H, Hedges LV, Valentine JC, eds (2009) The handbook of research synthesis and meta-analysis. Russell  
1578 Sage Foundation.
- 1579 Coopersmith J (2010) Energy, the subtle concept. The discovery of Feynman's blocks from Leibnitz to Einstein.  
1580 Oxford University Press:400 pp.
- 1581 Cummins J (1998) Mitochondrial DNA in mammalian reproduction. Rev Reprod 3:172-82.
- 1582 Dai Q, Shah AA, Garde RV, Yonish BA, Zhang L, Medvitz NA, Miller SE, Hansen EL, Dunn CN, Price TM  
1583 (2013) A truncated progesterone receptor (PR-M) localizes to the mitochondrion and controls cellular  
1584 respiration. Mol Endocrinol 27:741-53.
- 1585 Daum B, Walter A, Horst A, Osiewacz HD, Kühlbrandt W (2013) Age-dependent dissociation of ATP synthase  
1586 dimers and loss of inner-membrane cristae in mitochondria. Proc Natl Acad Sci U S A 110:15301-6.
- 1587 Divakaruni AS, Brand MD (2011) The regulation and physiology of mitochondrial proton leak. Physiology  
1588 (Bethesda) 26:192-205.
- 1589 Doerrier C, Garcia-Souza LF, Krumschnabel G, Wohlfarter Y, Mészáros AT, Gnaiger E (2018) High-Resolution  
1590 Fluorescence Respirometry and OXPHOS protocols for human cells, permeabilized fibres from small biopsies of  
1591 muscle, and isolated mitochondria. Methods Mol Biol 1782 (Palmeira CM, Moreno AJ, eds): Mitochondrial  
1592 Bioenergetics, 978-1-4939-7830-4.
- 1593 Doskey CM, van 't Erve TJ, Wagner BA, Buettner GR (2015) Moles of a substance per cell is a highly  
1594 informative dosing metric in cell culture. PLOS ONE 10:e0132572.
- 1595 Drahotová Z, Milerová M, Stieglarová A, Houstek J, Ostádal B (2004) Developmental changes of cytochrome *c*  
1596 oxidase and citrate synthase in rat heart homogenate. Physiol Res 53:119-22.
- 1597 Duarte FV, Palmeira CM, Rolo AP (2014) The role of microRNAs in mitochondria: small players acting wide.  
1598 Genes (Basel) 5:865-86.
- 1599 Ehinger JK, Morota S, Hansson MJ, Paul G, Elmér E (2015) Mitochondrial dysfunction in blood cells from  
1600 amyotrophic lateral sclerosis patients. J Neurol 262:1493-503.
- 1601 Ernster L, Schatz G (1981) Mitochondria: a historical review. J Cell Biol 91:227s-55s.
- 1602 Estabrook RW (1967) Mitochondrial respiratory control and the polarographic measurement of ADP:O ratios.  
1603 Methods Enzymol 10:41-7.
- 1604 Faber C, Zhu ZJ, Castellino S, Wagner DS, Brown RH, Peterson RA, Gates L, Barton J, Bickett M, Hagerty L,  
1605 Kimbrough C, Sola M, Bailey D, Jordan H, Elangbam CS (2014) Cardiolipin profiles as a potential  
1606 biomarker of mitochondrial health in diet-induced obese mice subjected to exercise, diet-restriction and  
1607 ephedrine treatment. J Appl Toxicol 34:1122-9.
- 1608 Feagin JE, Harrell MI, Lee JC, Coe KJ, Sands BH, Cannone JJ, Tami G, Schnare MN, Gutell RR (2012) The  
1609 fragmented mitochondrial ribosomal RNAs of *Plasmodium falciparum*. PLoS One 7:e38320.
- 1610 Fell D (1997) Understanding the control of metabolism. Portland Press.
- 1611 Forstner H, Gnaiger E (1983) Calculation of equilibrium oxygen concentration. In: Polarographic Oxygen  
1612 Sensors. Aquatic and Physiological Applications. Gnaiger E, Forstner H (eds), Springer, Berlin, Heidelberg,  
1613 New York:321-33.
- 1614 Garlid KD, Beavis AD, Ratkje SK (1989) On the nature of ion leaks in energy-transducing membranes. Biochim  
1615 Biophys Acta 976:109-20.
- 1616 Garlid KD, Semrad C, Zinchenko V. Does redox slip contribute significantly to mitochondrial respiration? In:  
1617 Schuster S, Rigoulet M, Ouhabi R, Mazat J-P, eds (1993) Modern trends in biothermokinetics. Plenum Press,  
1618 New York, London:287-93.
- 1619 Gerö D, Szabo C (2016) Glucocorticoids suppress mitochondrial oxidant production via upregulation of  
1620 uncoupling protein 2 in hyperglycemic endothelial cells. PLoS One 11:e0154813.
- 1621 Gnaiger E. Efficiency and power strategies under hypoxia. Is low efficiency at high glycolytic ATP production a  
1622 paradox? In: Surviving Hypoxia: Mechanisms of Control and Adaptation. Hochachka PW, Lutz PL, Sick T,  
1623 Rosenthal M, Van den Thillart G, eds (1993a) CRC Press, Boca Raton, Ann Arbor, London, Tokyo:77-109.
- 1624 Gnaiger E (1993b) Nonequilibrium thermodynamics of energy transformations. Pure Appl Chem 65:1983-2002.

- 1625 Gnaiger E (2001) Bioenergetics at low oxygen: dependence of respiration and phosphorylation on oxygen and  
 1626 adenosine diphosphate supply. *Respir Physiol* 128:277-97.
- 1627 Gnaiger E (2009) Capacity of oxidative phosphorylation in human skeletal muscle. New perspectives of  
 1628 mitochondrial physiology. *Int J Biochem Cell Biol* 41:1837-45.
- 1629 Gnaiger E (2014) Mitochondrial pathways and respiratory control. An introduction to OXPHOS analysis. 4th ed.  
 1630 Mitochondr Physiol Network 19.12. Oroboros MiPNet Publications, Innsbruck:80 pp.
- 1631 Gnaiger E, Méndez G, Hand SC (2000) High phosphorylation efficiency and depression of uncoupled respiration  
 1632 in mitochondria under hypoxia. *Proc Natl Acad Sci USA* 97:11080-5.
- 1633 Greggio C, Jha P, Kulkarni SS, Lagarrigue S, Broskey NT, Boutant M, Wang X, Conde Alonso S, Ofori E,  
 1634 Auwerx J, Cantó C, Amati F (2017) Enhanced respiratory chain supercomplex formation in response to  
 1635 exercise in human skeletal muscle. *Cell Metab* 25:301-11.
- 1636 Hinkle PC (2005) P/O ratios of mitochondrial oxidative phosphorylation. *Biochim Biophys Acta* 1706:1-11.
- 1637 Hofstadter DR (1979) Gödel, Escher, Bach: An eternal golden braid. A metaphorical fugue on minds and  
 1638 machines in the spirit of Lewis Carroll. Harvester Press:499 pp.
- 1639 Illaste A, Laasmaa M, Peterson P, Vendelin M (2012) Analysis of molecular movement reveals latticelike  
 1640 obstructions to diffusion in heart muscle cells. *Biophys J* 102:739-48.
- 1641 Jasienski M, Bazzaz FA (1999) The fallacy of ratios and the testability of models in biology. *Oikos* 84:321-26.
- 1642 Jepihhina N, Beraud N, Sepp M, Birkedal R, Vendelin M (2011) Permeabilized rat cardiomyocyte response  
 1643 demonstrates intracellular origin of diffusion obstacles. *Biophys J* 101:2112-21.
- 1644 Karnkowska A, Vacek V, Zubáčová Z, Treitli SC, Petrželková R, Eme L, Novák L, Žárský V, Barlow LD,  
 1645 Herman EK, Soukal P, Hroudová M, Doležal P, Stairs CW, Roger AJ, Eliáš M, Dacks JB, Vlček Č, Hampl V  
 1646 (2016) A eukaryote without a mitochondrial organelle. *Curr Biol* 26:1274-84.
- 1647 Klepinin A, Ounpuu L, Guzun R, Chekulayev V, Timohhina N, Tepp K, Shevchuk I, Schlattner U, Kaambre T  
 1648 (2016) Simple oxygraphic analysis for the presence of adenylate kinase 1 and 2 in normal and tumor cells. *J*  
 1649 *Bioenerg Biomembr* 48:531-48.
- 1650 Klingenberg M (2017) UCP1 - A sophisticated energy valve. *Biochimie* 134:19-27.
- 1651 Koit A, Shevchuk I, Ounpuu L, Klepinin A, Chekulayev V, Timohhina N, Tepp K, Puurand M, Truu L, Heck K,  
 1652 Valvere V, Guzun R, Kaambre T (2017) Mitochondrial respiration in human colorectal and breast cancer  
 1653 clinical material is regulated differently. *Oxid Med Cell Longev* 1372640.
- 1654 Komlódi T, Tretter L (2017) Methylene blue stimulates substrate-level phosphorylation catalysed by succinyl-  
 1655 CoA ligase in the citric acid cycle. *Neuropharmacology* 123:287-98.
- 1656 Korn E (1969) Cell membranes: structure and synthesis. *Annu Rev Biochem* 38:263-88.
- 1657 Lai N, M Kummitha C, Rosca MG, Fujioka H, Tandler B, Hoppel CL (2018) Isolation of mitochondrial  
 1658 subpopulations from skeletal muscle: optimizing recovery and preserving integrity. *Acta Physiol*  
 1659 (Oxf):e13182. doi: 10.1111/apha.13182.
- 1660 Lane N (2005) Power, sex, suicide: mitochondria and the meaning of life. Oxford University Press:354 pp.
- 1661 Larsen S, Nielsen J, Neigaard Nielsen C, Nielsen LB, Wibrand F, Stride N, Schroder HD, Boushel RC, Helge  
 1662 JW, Dela F, Hey-Mogensen M (2012) Biomarkers of mitochondrial content in skeletal muscle of healthy  
 1663 young human subjects. *J Physiol* 590:3349-60.
- 1664 Lee C, Zeng J, Drew BG, Sallam T, Martin-Montalvo A, Wan J, Kim SJ, Mehta H, Hevener AL, de Cabo R,  
 1665 Cohen P (2015) The mitochondrial-derived peptide MOTS-c promotes metabolic homeostasis and reduces  
 1666 obesity and insulin resistance. *Cell Metab* 21:443-54.
- 1667 Lee SR, Kim HK, Song IS, Youm J, Dizon LA, Jeong SH, Ko TH, Heo HJ, Ko KS, Rhee BD, Kim N, Han J  
 1668 (2013) Glucocorticoids and their receptors: insights into specific roles in mitochondria. *Prog Biophys Mol*  
 1669 *Biol* 112:44-54.
- 1670 Leek BT, Mudaliar SR, Henry R, Mathieu-Costello O, Richardson RS (2001) Effect of acute exercise on citrate  
 1671 synthase activity in untrained and trained human skeletal muscle. *Am J Physiol Regul Integr Comp Physiol*  
 1672 280:R441-7.
- 1673 Lemieux H, Blier PU, Gnaiger E (2017) Remodeling pathway control of mitochondrial respiratory capacity by  
 1674 temperature in mouse heart: electron flow through the Q-junction in permeabilized fibers. *Sci Rep* 7:2840.
- 1675 Lenaz G, Tioli G, Falasca AI, Genova ML (2017) Respiratory supercomplexes in mitochondria. In: Mechanisms  
 1676 of primary energy trasduction in biology. M Wikstrom (ed) Royal Society of Chemistry Publishing, London,  
 1677 UK:296-337.
- 1678 Liu S, Roellig DM, Guo Y, Li N, Frace MA, Tang K, Zhang L, Feng Y, Xiao L (2016) Evolution of mitosome  
 1679 metabolism and invasion-related proteins in *Cryptosporidium*. *BMC Genomics* 17:1006.
- 1680 Margulis L (1970) Origin of eukaryotic cells. New Haven: Yale University Press.
- 1681 Meinild Lundby AK, Jacobs RA, Gehrig S, de Leur J, Hauser M, Bonne TC, Flück D, Dandanell S, Kirk N,  
 1682 Kaech A, Ziegler U, Larsen S, Lundby C (2018) Exercise training increases skeletal muscle mitochondrial  
 1683 volume density by enlargement of existing mitochondria and not de novo biogenesis. *Acta Physiol* 222,  
 1684 e12905.

- 1685 Menshikova EV, Ritov VB, Fairfull L, Ferrell RE, Kelley DE, Goodpaster BH (2006) Effects of exercise on  
1686 mitochondrial content and function in aging human skeletal muscle. *J Gerontol A Biol Sci Med Sci* 61:534-  
1687 40.
- 1688 Menshikova EV, Ritov VB, Ferrell RE, Azuma K, Goodpaster BH, Kelley DE (2007) Characteristics of skeletal  
1689 muscle mitochondrial biogenesis induced by moderate-intensity exercise and weight loss in obesity. *J Appl*  
1690 *Physiol* (1985) 103:21-7.
- 1691 Menshikova EV, Ritov VB, Toledo FG, Ferrell RE, Goodpaster BH, Kelley DE (2005) Effects of weight loss  
1692 and physical activity on skeletal muscle mitochondrial function in obesity. *Am J Physiol Endocrinol Metab*  
1693 288:E818-25.
- 1694 Miller GA (1991) *The science of words*. Scientific American Library New York:276 pp.
- 1695 Mitchell P (1961) Coupling of phosphorylation to electron and hydrogen transfer by a chemi-osmotic type of  
1696 mechanism. *Nature* 191:144-8.
- 1697 Mitchell P (2011) Chemiosmotic coupling in oxidative and photosynthetic phosphorylation. *Biochim Biophys*  
1698 *Acta Bioenergetics* 1807:1507-38.
- 1699 Mogensen M, Sahlin K, Fernström M, Glintborg D, Vind BF, Beck-Nielsen H, Højlund K (2007) Mitochondrial  
1700 respiration is decreased in skeletal muscle of patients with type 2 diabetes. *Diabetes* 56:1592-9.
- 1701 Mohr PJ, Phillips WD (2015) Dimensionless units in the SI. *Metrologia* 52:40-7.
- 1702 Moreno M, Giacco A, Di Munno C, Goglia F (2017) Direct and rapid effects of 3,5-diiodo-L-thyronine (T2).  
1703 *Mol Cell Endocrinol* 7207:30092-8.
- 1704 Morrow RM, Picard M, Derbeneva O, Leipzig J, McManus MJ, Gousspillou G, Barbat-Artigas S, Dos Santos C,  
1705 Hepple RT, Murdock DG, Wallace DC (2017) Mitochondrial energy deficiency leads to hyperproliferation of  
1706 skeletal muscle mitochondria and enhanced insulin sensitivity. *Proc Natl Acad Sci U S A* 114:2705-10.
- 1707 Murley A, Nunnari J (2016) The emerging network of mitochondria-organelle contacts. *Mol Cell* 61:648-53.
- 1708 National Academies of Sciences, Engineering, and Medicine (2018) International coordination for science data  
1709 infrastructure: Proceedings of a workshop—in brief. Washington, DC: The National Academies Press. doi:  
1710 <https://doi.org/10.17226/25015>.
- 1711 Oemer G, Lackner L, Muigg K, Krumschnabel G, Watschinger K, Sailer S, Lindner H, Gnaiger E, Wortmann  
1712 SB, Werner ER, Zschocke J, Keller MA (2018) The molecular structural diversity of mitochondrial  
1713 cardiolipins. *Proc Natl Acad Sci U S A* 115:4158-63.
- 1714 Palmfeldt J, Bross P (2017) Proteomics of human mitochondria. *Mitochondrion* 33:2-14.
- 1715 Paradies G, Paradies V, De Benedictis V, Ruggiero FM, Petrosillo G (2014) Functional role of cardiolipin in  
1716 mitochondrial bioenergetics. *Biochim Biophys Acta* 1837:408-17.
- 1717 Pesta D, Gnaiger E (2012) High-Resolution Respirometry. OXPHOS protocols for human cells and  
1718 permeabilized fibres from small biopsies of human muscle. *Methods Mol Biol* 810:25-58.
- 1719 Pesta D, Hoppel F, Macek C, Messner H, Faulhaber M, Kobel C, Parson W, Burtscher M, Schocke M, Gnaiger  
1720 E (2011) Similar qualitative and quantitative changes of mitochondrial respiration following strength and  
1721 endurance training in normoxia and hypoxia in sedentary humans. *Am J Physiol Regul Integr Comp Physiol*  
1722 301:R1078-87.
- 1723 Price TM, Dai Q (2015) The role of a mitochondrial progesterone receptor (PR-M) in progesterone action.  
1724 *Semin Reprod Med* 33:185-94.
- 1725 Puchowicz MA, Varnes ME, Cohen BH, Friedman NR, Kerr DS, Hoppel CL (2004) Oxidative phosphorylation  
1726 analysis: assessing the integrated functional activity of human skeletal muscle mitochondria – case studies.  
1727 *Mitochondrion* 4:377-85. Puntschart A, Claassen H, Jostarndt K, Hoppeler H, Billeter R (1995) mRNAs of  
1728 enzymes involved in energy metabolism and mtDNA are increased in endurance-trained athletes. *Am J*  
1729 *Physiol* 269:C619-25.
- 1730 Quiros PM, Mottis A, Auwerx J (2016) Mitonuclear communication in homeostasis and stress. *Nat Rev Mol*  
1731 *Cell Biol* 17:213-26.
- 1732 Rackham O, Mercer TR, Filipovska A (2012) The human mitochondrial transcriptome and the RNA-binding  
1733 proteins that regulate its expression. *WIREs RNA* 3:675-95.
- 1734 Reichmann H, Hoppeler H, Mathieu-Costello O, von Bergen F, Pette D (1985) Biochemical and ultrastructural  
1735 changes of skeletal muscle mitochondria after chronic electrical stimulation in rabbits. *Pflugers Arch* 404:1-  
1736 9.
- 1737 Renner K, Amberger A, Konwalinka G, Gnaiger E (2003) Changes of mitochondrial respiration, mitochondrial  
1738 content and cell size after induction of apoptosis in leukemia cells. *Biochim Biophys Acta* 1642:115-23.
- 1739 Rice DW, Alverson AJ, Richardson AO, Young GJ, Sanchez-Puerta MV, Munzinger J, Barry K, Boore JL,  
1740 Zhang Y, dePamphilis CW, Knox EB, Palmer JD (2016) Horizontal transfer of entire genomes via  
1741 mitochondrial fusion in the angiosperm *Amborella*. *Science* 342:1468-73.
- 1742 Rich P (2003) Chemiosmotic coupling: The cost of living. *Nature* 421:583.
- 1743 Rich PR (2013) Chemiosmotic theory. *Encyclopedia Biol Chem* 1:467-72.
- 1744 Roger JA, Munoz-Gomes SA, Kamikawa R (2017) The origin and diversification of mitochondria. *Curr Biol*  
1745 27:R1177-92.

- 1746 Rostovtseva TK, Sheldon KL, Hassanzadeh E, Monge C, Saks V, Bezrukov SM, Sackett DL (2008) Tubulin  
 1747 binding blocks mitochondrial voltage-dependent anion channel and regulates respiration. *Proc Natl Acad Sci*  
 1748 *USA* 105:18746-51.
- 1749 Rustin P, Parfait B, Chretien D, Bourgeron T, Djouadi F, Bastin J, Rötig A, Munnich A (1996) Fluxes of  
 1750 nicotinamide adenine dinucleotides through mitochondrial membranes in human cultured cells. *J Biol Chem*  
 1751 271:14785-90.
- 1752 Saks VA, Veksler VI, Kuznetsov AV, Kay L, Sikk P, Tiivel T, Tranqui L, Olivares J, Winkler K, Wiedemann F,  
 1753 Kunz WS (1998) Permeabilised cell and skinned fiber techniques in studies of mitochondrial function in  
 1754 vivo. *Mol Cell Biochem* 184:81-100.
- 1755 Salabei JK, Gibb AA, Hill BG (2014) Comprehensive measurement of respiratory activity in permeabilized cells  
 1756 using extracellular flux analysis. *Nat Protoc* 9:421-38.
- 1757 Sazanov LA (2015) A giant molecular proton pump: structure and mechanism of respiratory complex I. *Nat Rev*  
 1758 *Mol Cell Biol* 16:375-88.
- 1759 Schneider TD (2006) Claude Shannon: biologist. The founder of information theory used biology to formulate  
 1760 the channel capacity. *IEEE Eng Med Biol Mag* 25:30-3.
- 1761 Schönfeld P, Dymkowska D, Wojtczak L (2009) Acyl-CoA-induced generation of reactive oxygen species in  
 1762 mitochondrial preparations is due to the presence of peroxisomes. *Free Radic Biol Med* 47:503-9.
- 1763 Schultz J, Wiesner RJ (2000) Proliferation of mitochondria in chronically stimulated rabbit skeletal muscle--  
 1764 transcription of mitochondrial genes and copy number of mitochondrial DNA. *J Bioenerg Biomembr* 32:627-  
 1765 34.
- 1766 Speijer D (2016) Being right on Q: shaping eukaryotic evolution. *Biochem J* 473:4103-27.
- 1767 Sugiura A, Mattie S, Prudent J, McBride HM (2017) Newly born peroxisomes are a hybrid of mitochondrial and  
 1768 ER-derived pre-peroxisomes. *Nature* 542:251-4.
- 1769 Simson P, Jepihhina N, Laasmaa M, Peterson P, Birkedal R, Vendelin M (2016) Restricted ADP movement in  
 1770 cardiomyocytes: Cytosolic diffusion obstacles are complemented with a small number of open mitochondrial  
 1771 voltage-dependent anion channels. *J Mol Cell Cardiol* 97:197-203.
- 1772 Stucki JW, Ineichen EA (1974) Energy dissipation by calcium recycling and the efficiency of calcium transport  
 1773 in rat-liver mitochondria. *Eur J Biochem* 48:365-75.
- 1774 Tonkonogi M, Harris B, Sahlin K (1997) Increased activity of citrate synthase in human skeletal muscle after a  
 1775 single bout of prolonged exercise. *Acta Physiol Scand* 161:435-6.
- 1776 Torralba D, Baixauli F, Sánchez-Madrid F (2016) Mitochondria know no boundaries: mechanisms and functions  
 1777 of intercellular mitochondrial transfer. *Front Cell Dev Biol* 4:107. eCollection 2016.
- 1778 Vamecq J, Schepers L, Parmentier G, Mannaerts GP (1987) Inhibition of peroxisomal fatty acyl-CoA oxidase by  
 1779 antimycin A. *Biochem J* 248:603-7.
- 1780 Waczulikova I, Habodaszova D, Cagalinec M, Ferko M, Ulicna O, Mateasik A, Sikurova L, Ziegelhöffer A  
 1781 (2007) Mitochondrial membrane fluidity, potential, and calcium transients in the myocardium from acute  
 1782 diabetic rats. *Can J Physiol Pharmacol* 85:372-81.
- 1783 Wagner BA, Venkataraman S, Buettner GR (2011) The rate of oxygen utilization by cells. *Free Radic Biol Med*  
 1784 51:700-712.
- 1785 Wang H, Hiatt WR, Barstow TJ, Brass EP (1999) Relationships between muscle mitochondrial DNA content,  
 1786 mitochondrial enzyme activity and oxidative capacity in man: alterations with disease. *Eur J Appl Physiol*  
 1787 *Occup Physiol* 80:22-7.
- 1788 Watt IN, Montgomery MG, Runswick MJ, Leslie AG, Walker JE (2010) Bioenergetic cost of making an  
 1789 adenosine triphosphate molecule in animal mitochondria. *Proc Natl Acad Sci U S A* 107:16823-7.
- 1790 Weibel ER, Hoppeler H (2005) Exercise-induced maximal metabolic rate scales with muscle aerobic capacity. *J*  
 1791 *Exp Biol* 208:1635-44.
- 1792 White DJ, Wolff JN, Pierson M, Gemmell NJ (2008) Revealing the hidden complexities of mtDNA inheritance.  
 1793 *Mol Ecol* 17:4925-42.
- 1794 Wikström M, Hummer G (2012) Stoichiometry of proton translocation by respiratory complex I and its  
 1795 mechanistic implications. *Proc Natl Acad Sci U S A* 109:4431-6.
- 1796 Williams EG, Wu Y, Jha P, Dubuis S, Blattmann P, Argmann CA, Houten SM, Amariuta T, Wolski W,  
 1797 Zamboni N, Aebersold R, Auwerx J (2016) Systems proteomics of liver mitochondria function. *Science* 352  
 1798 (6291):aad0189
- 1799 Willis WT, Jackman MR, Messer JI, Kuzmiak-Glancy S, Glancy B (2016) A simple hydraulic analog model of  
 1800 oxidative phosphorylation. *Med Sci Sports Exerc* 48:990-1000.
- 1801 Zíková A, Hampl V, Paris Z, Týč J, Lukeš J (2016) Aerobic mitochondria of parasitic protists: diverse genomes  
 1802 and complex functions. *Mol Biochem Parasitol* 209:46-57.
- 1803
- 1804

## 1805 Supplement

1806

### 1807 S1. Manuscript phases and versions - an open-access approach

1808

1809 This manuscript on ‘Mitochondrial respiratory states and rates’ is a position statement in the frame of COST Action  
1810 CA15203 MitoEAGLE. The list of co-authors evolved beyond phase 1 in the bottom-up spirit of COST.

1811 The global MitoEAGLE network made it possible to collaborate with a large number of co-authors to reach  
1812 consensus on the present manuscript. Nevertheless, we do not consider scientific progress to be supported by  
1813 ‘declaration’ statements (other than on ethical or political issues). Our manuscript aims at providing arguments for  
1814 further debate rather than pushing opinions. We hope to initiate a much broader process of discussion and want to  
1815 raise the awareness on the importance of a consistent terminology for reporting of scientific data in the field of  
1816 bioenergetics, mitochondrial physiology and pathology. Quality of research requires quality of communication.  
1817 Some established researchers in the field may not want to re-consider the use of jargon which has become  
1818 established despite deficiencies of accuracy and meaning. In the long run, superior standards will become accepted.  
1819 We hope to contribute to this evolutionary process, with an emphasis on harmonization rather than standardization.

1820 *Phase 1* The protonmotive force and respiratory control

1821 [http://www.mitoeagle.org/index.php/The\\_protonmotive\\_force\\_and\\_respiratory\\_control](http://www.mitoeagle.org/index.php/The_protonmotive_force_and_respiratory_control)

1822 • 2017-04-09 to 2017-09-18 (44 versions)

1823 • 2017-09-21 to 2018-02-06 (21 versions)

1824 [http://www.mitoeagle.org/index.php/MitoEAGLE\\_preprint\\_2017-09-21](http://www.mitoeagle.org/index.php/MitoEAGLE_preprint_2017-09-21)

1825 2017-11-11: Print version (16) for MiP2017/MitoEAGLE conference in Hradec Kralove

1826 *Phase 2* Mitochondrial respiratory states and rates: Building blocks of mitochondrial physiology Part 1

1827 [http://www.mitoeagle.org/index.php/MitoEAGLE\\_preprint\\_2018-02-08](http://www.mitoeagle.org/index.php/MitoEAGLE_preprint_2018-02-08)

1828 • 2018-02-08 – (42 Versions up to 2018-09-24)

1829 *Phase 3* Submission to a preprint server: [BioRxiv](https://www.biorxiv.org/)

1830 *Phase 4* Journal submission

1831 CELL METABOLISM, aiming at indexing by *The Web of Science* and *PubMed*. We expect feedback from  
1832 many colleagues until the end of May, to prepare a final circular to all co-authors in June 2018.

1833

1834

## 1835 S2. Authors

1836

1837 This manuscript developed as an open invitation to scientists and students to join as co-authors, to provide a  
1838 balanced view on mitochondrial respiratory control and a consensus statement on reporting data of mitochondrial  
1839 respiration in terms of metabolic flows and fluxes.

1840 Co-authors are added in alphabetical order based upon a first draft written by the corresponding author, who  
1841 edited all versions. *Co-authors confirm to have read the final manuscript, possibly have made additions or*  
1842 *suggestions for improvement, and agree to implement the recommendations into future manuscripts, presentations*  
1843 *and teaching materials.*

1844 We continue to invite comments and suggestions, particularly if you are an early career investigator adding  
1845 an open future-oriented perspective, or an established scientist providing a balanced historical basis. Your critical  
1846 input into the quality of the manuscript will be most welcome, improving our aims to be educational, general,  
1847 consensus-oriented, and practically helpful for students working in mitochondrial respiratory physiology.

1848 To join as a co-author, please feel free to focus on a particular section, providing direct input and references,  
1849 and contributing to the scope of the manuscript from the perspective of your expertise. Your comments will be  
1850 largely posted on the discussion page of the MitoEAGLE preprint website.

1851 If you prefer to submit comments in the format of a referee's evaluation rather than a contribution as a co-  
1852 author, we will be glad to distribute your views to the updated list of co-authors for a balanced response. We would  
1853 ask for your consent on this open bottom-up policy.

1854

1855

## 1856 S3. Joining COST Actions

1857

1858 • CA15203 MitoEAGLE - [http://www.cost.eu/COST\\_Actions/ca/CA15203](http://www.cost.eu/COST_Actions/ca/CA15203)

1859 • CA16225 EU-CARDIOPROTECTION - [http://www.cost.eu/COST\\_Actions/ca/CA16225](http://www.cost.eu/COST_Actions/ca/CA16225)

1860 • CA17129 CardioRNA - [http://www.cost.eu/COST\\_Actions/ca/CA17129](http://www.cost.eu/COST_Actions/ca/CA17129)



# Mitochondrial respiratory states and rates:



## Building blocks of mitochondrial physiology

Part 1 - [www.mitoeagle.org/index.php/MitoEAGLE\\_preprint\\_2018-02-08](http://www.mitoeagle.org/index.php/MitoEAGLE_preprint_2018-02-08)

Gnaiger E<sup>1,2</sup>, corresponding author  
355 co-authors, MitoEAGLE Working Group

<sup>1</sup>Medical University Innsbruck  
<sup>2</sup>Oroboros, Innsbruck, Austria

**Aims** Clarity of concept and consistency of nomenclature facilitate effective transdisciplinary communication, education, and ultimately further discovery.

Adhering to uniform standards and harmonizing the terminology concerning mitochondrial respiratory states and rates will support the development of databases of mitochondrial respiratory function in cells, tissues, and species.

**Summary** Recommendations on coupling control states and rates are focused on studies with mitochondrial preparations.

**Fig. 1:** Respiration is defined by O<sub>2</sub> flux balance.  
**Fig. 2:** OXPHOS analysis is based on the study of mt- preparations. Metabolic fluxes measured in defined coupling and pathway control states provide insights into the meaning of cellular respiration.  
**Fig. 3:** Interpretation of respiratory rates depends critically on appropriate normalization.

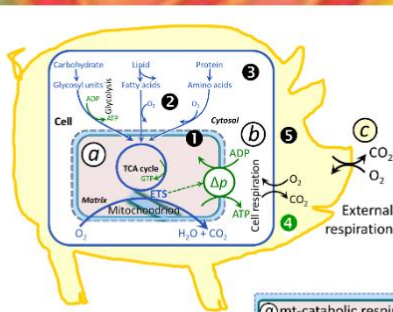
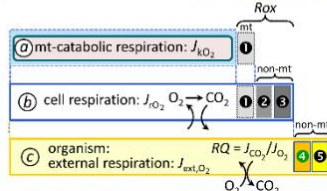


**Figure 1. From mitochondrial to external respiration**

Mitochondrial (mt) respiration is the oxidation of fuel substrates (electron donors) and reduction of O<sub>2</sub> catalysed by the electron transfer system, ETS:

- a** mt-catabolic respiration, excluding
- 1** mt-residual oxygen consumption, *Rox*.
- b** Total cellular O<sub>2</sub> consumption, including mt-*Rox*, **e** non-mt catabolic *Rox*, particularly by peroxisomal oxidases, and **e** non-mt *Rox* unrelated to catabolism.
- c** External respiration, including **1** aerobic microbial respiration, and **2** extracellular O<sub>2</sub> consumption.



MIPart by Odra Noel

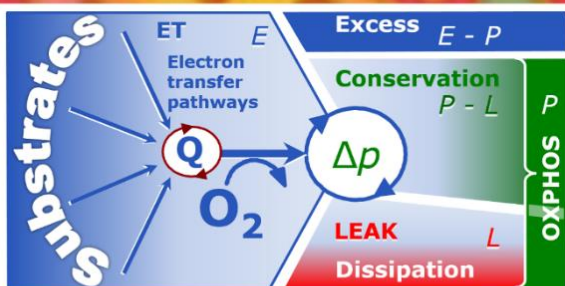


**Figure 2. Respiratory states (ET, OXPHOS, LEAK) and corresponding rates (E, P, L)**

Net OXPHOS-capacity, *P-L*, and excess capacity, *E-P*.  
Table 1. Coupling states and residual oxygen consumption in mitochondrial preparations in relation to respiration- and phosphorylation-flux, *J<sub>ko</sub>*, and *J<sub>p</sub>*, and protonmotive force,  $\Delta p$ . Coupling states are established at kinetically-saturating concentrations of fuel substrates and O<sub>2</sub>.

State	<i>J<sub>ko</sub></i>	<i>J<sub>p</sub></i>	$\Delta p$	Inducing factors	Limiting factors
LEAK	<i>L</i> ; low, cation leak-dependent respiration	0	max.	proton leak, slip, and cation cycling	<i>J<sub>p</sub></i> = 0: (1) without ADP, <i>L<sub>sc</sub></i> ; (2) max. ATP/ADP ratio, <i>L<sub>r</sub></i> ; or (3) inhibition of the phosphorylation-pathway, <i>L<sub>only</sub></i>
OXPHOS	<i>P</i> ; high, ADP-stimulated respiration	max.	high	kinetically-saturating [ADP] and [P <sub>i</sub> ]	<i>J<sub>p</sub></i> , by phosphorylation-pathway; or <i>J<sub>ko</sub></i> , by ET-capacity
ET	<i>E</i> ; max., noncoupled respiration	0	low	optimal external uncoupler concentration for max. <i>J<sub>O<sub>2</sub>E</sub></i>	<i>J<sub>ko</sub></i> , by ET-capacity
ROX	<i>Rox</i> ; min., residual O <sub>2</sub> consumption	0	0	<i>J<sub>O<sub>2</sub>Rox</sub></i> in non-ET-pathway oxidation reactions	inhibition of all ET-pathways; or absence of fuel substrates

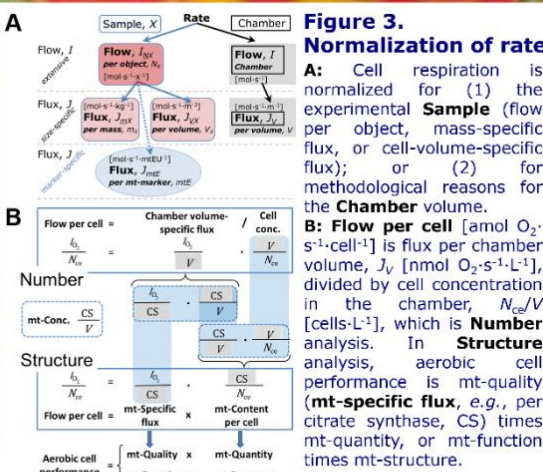


**Figure 3. Normalization of rate**

**A:** Cell respiration is normalized for (1) the experimental **Sample** (flow per object, mass-specific flux), or cell-volume-specific flux; or (2) for methodological reasons for the **Chamber** volume.  
**B:** Flow per cell [amol O<sub>2</sub> s<sup>-1</sup> cell<sup>-1</sup>] is flux per chamber volume, *J<sub>v</sub>* [nmol O<sub>2</sub> s<sup>-1</sup> L<sup>-1</sup>], divided by cell concentration in the chamber, *N<sub>ce</sub>*/V [cells L<sup>-1</sup>], which is **Number** analysis. In **Structure** analysis, aerobic cell performance is mt-quality (mt-specific flux, e.g., per citrate synthase, CS) times mt-quantity, or mt-function times mt-structure.

# COST Action CA15203 MitoEAGLE

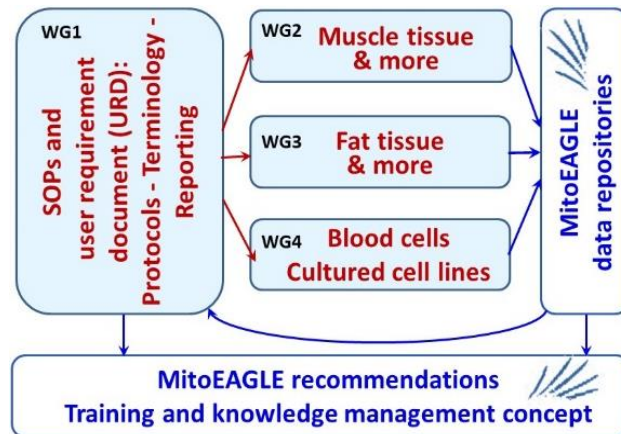
Evolution Age Gender  
Lifestyle Environment



## Mission of the global MitoEAGLE network

in collaboration with the Mitochondrial Physiology Society, MiPs

- Improve our knowledge on mitochondrial function in health and disease with regard to Evolution, Age, Gender, Lifestyle and Environment
- Interrelate studies across laboratories with the help of a MitoEAGLE data management system
- Provide standardized measures to link mitochondrial and physiological performance to understand the myriad of factors that play a role in mitochondrial physiology



Join the COST Action MitoEAGLE - contribute to the quality management network.



More information:  
[www.mitoeagle.org](http://www.mitoeagle.org)



Funded by the Horizon 2020 Framework Programme  
of the European Union

